

**ISTANBUL TECHNICAL UNIVERSITY ★ GRADUATE SCHOOL OF SCIENCE**  
**ENGINEERING AND TECHNOLOGY**

**AN AUTOMATION OF HIGH VOLTAGE IMPULSE GENERATOR**

**M. Sc. THESIS**

**Farid ABDOLALIZADEHGHAREHVERAN**

**Department of Electrical Engineering**

**Electrical Engineering Programme**

**MAY 2013**



**ISTANBUL TECHNICAL UNIVERSITY ★ GRADUATE SCHOOL OF SCIENCE**  
**ENGINEERING AND TECHNOLOGY**

**AN AUTOMATION OF HIGH VOLTAGE IMPULSE GENERATOR**

**M. Sc. THESIS**

**Farid ABDOLALIZADEHGHAREHVERAN**  
**(504091083)**

**Department of Electrical Engineering**

**Electrical Engineering Programme**

**Thesis Advisor: Prof. Dr. Aydođan ÖZDEMİR**

**MAY 2013**



**İSTANBUL TEKNİK ÜNİVERSİTESİ ★ FEN BİLİMLERİ ENSTİTÜSÜ**

**YÜKSEK DARBE GERİLİMİ ÜRETECİNİN OTOMASYONU**

**YÜKSEK LİSANS TEZİ**

**Farid ABDOLALIZADEHGHAREHVERAN  
(504091083)**

**Elektrik Mühendisliği Anabilim Dalı**

**Elektrik Mühendisliği Programı**

**Tez Danışmanı: Prof. Dr. Aydoğan ÖZDEMİR**

**MAYIS 2013**



**Farid Abdolalizadehgharehveran**, a **M. Sc.** student of ITU **Graduate School of SCIENCE ENGINEERING AND TECHNOLOGY** student ID 504091083, successfully defended the **thesis** entitled “**AN AUTOMATION OF HIGH VOLTAGE IMPULSE GENERATOR**”, which he prepared after fulfilling the requirements specified in the associated legislations, before the jury whose signatures are below.

**Thesis Advisor :**      **Prof. Dr. Aydođan ÖZDEMİR**      .....

Istanbul Technical University

**Jury Members :**      **Prof. Dr. Özcan KALENDERLİ**      .....

Istanbul Technical University

**Prof. Dr. Mukden UĞUR**      .....

Istanbul University

**Date of Submission : 19 November 2012**

**Date of Defense : 5 MAY 2013**





*“Anama ki dil onundur, Atama ki toprak onundur*

*Eşime ki hayatım onundur... “*



## **FOREWORD**

It is safe to say that studying in Istanbul Technical University was my best experience in whole my studying life and as my own opinion it is because of great Turk nation. It was all friendly and warm all communities in university and social life in TURKEY.

I would like to thank a lot of name here that helped me during thesis to make it done. First of all I would express gratitude to my supervisor Prof. Dr. Aydoğan ÖZDEMİR for his helpful instructions and patient during thesis. My thanks go to research assistance Suat İLHAN, Alparslan ZEHİR and Emrah DOKUR, for their assists during tests in laboratory. Thanks to Yasin, Yahya and all staffs of FUAT KULUNK High Voltage Laboratory of Istanbul Technical University that they made me feel free in utilizing all facilities in laboratory. I would express gratitude to my teachers and academic staffs of Electrical Engineering Department of Istanbul Technical University especially Prof. Dr. Özcan KALENDERLİ that I learnt a lot of him during my master study.

Finally I would express my great gratitude to my wife, Forugh that it was impossible to do all this without her supports and my great family. I would never receive anything better than my parents gave it to me.

November 2012

Farid ABDOLALİZADEHGHAREHVERAN  
Electrical Engineer



## TABLE OF CONTENTS

	<u>Page</u>
<b>FOREWORD</b> .....	<b>ix</b>
<b>TABLE OF CONTENTS</b> .....	<b>xi</b>
<b>ABBREVIATIONS</b> .....	<b>xiii</b>
<b>LIST OF TABLES</b> .....	<b>xv</b>
<b>LIST OF FIGURES</b> .....	<b>xvii</b>
<b>SUMMARY</b> .....	<b>xix</b>
<b>ÖZET</b> .....	<b>xxiii</b>
<b>1. INTRODUCTION</b> .....	<b>1</b>
<b>2. OVERVOLTAGES IN POWER SYSTEM</b> .....	<b>5</b>
2.1 Overvoltages in the System.....	5
2.1.1 Standard switching overvoltages.....	6
2.1.2 Standard lightning overvoltages.....	7
2.1.3 Front chopped lightning impulse voltage.....	9
2.1.4 Tail chopped lightning impulse voltage.....	9
2.2 Overvoltages Effect on Power System.....	10
2.3 High Voltage Tests.....	11
2.4 Impulse Voltage Generating Circuits.....	12
2.5 Multistage Impulse Generators .....	18
2.6 Fencing the Test Area.....	21
2.7 Earthing Equipment.....	22
2.8 Shielding.....	25
<b>3. MEASUREMENT OF IMPULSE VOLTAGES</b> .....	<b>27</b>
3.1 General Aspect of Measurement .....	27
3.2 Measurement of Impulse Voltages.....	28
3.3 Considerations in Impulse Voltage Measuring .....	30
3.4 Transfer Characteristics.....	31
3.5 Unit Step Response .....	34
<b>4. TRIGGERING SYSTEM OF IVG</b> .....	<b>39</b>
4.1 Trigatron.....	39
4.2 Mathematical Aspect of Trigatron System.....	43
<b>5. AUTOMATION OF IMPULSE VOLTAGE GENERATOR</b> .....	<b>51</b>
5.1 Aim of Automation .....	51
5.2 Definition of “ $u_{tr}$ ” Parameter.....	53
5.3 Proper Operation of IVG.....	54
5.4 Trigatron Setup for IVG.....	55
5.5 Triggering Pulse Generation .....	56
5.6 Trigatron Test.....	58
5.7 Test Results .....	59
5.8 Trigger Pulse Magnitude and Energy Effect on Trigatron Operation.....	62
5.8.1 Trigger pulse magnitude .....	62
5.8.2 Trigger pulse energy .....	63
5.9 Unit Step Response of Impulse Voltage Divider .....	66

5.9.1 Full divider unit step response .....	67
5.9.2 Half divider unit step response .....	69
<b>6. CONCLUSION.....</b>	<b>72</b>
6.1 Conclusion.....	72
<b>REFERENCES .....</b>	<b>75</b>
<b>CURRICULUM VITAE.....</b>	<b>77</b>

## **ABBREVIATIONS**

<b>AC</b>	: Alternative Current
<b>BIL</b>	: Basic Insulating Level
<b>BSL</b>	: Basic Switching Impulse Insulation Level
<b>C</b>	: Capacitor
<b>CG</b>	: Cloud to Ground
<b>DC</b>	: Direct Current
<b>ESS</b>	: Error sum-of-squares
<b>HV</b>	: High Voltage
<b>IC</b>	: Intra Cloud
<b>IVG</b>	: Impulse Voltage Generator
<b>IV</b>	: Impulse Voltage
<b>IVD</b>	: Impulse Voltage Divider
<b>ITU</b>	: Istanbul Technical University
<b>kV</b>	: Kilo Volt
<b>LV</b>	: Low Voltage
<b>MHz</b>	: Mega Hertz
<b>MV</b>	: Mega Volt
<b>MVA</b>	: Mega Volt Ampere
<b>MW</b>	: Mega Watt
<b>USR</b>	: Unit Step Response





## LIST OF TABLES

	<u>Page</u>
<b>Table 2.1</b> : Dielectric strength of some materials.....	10
<b>Table 5.1</b> : Test results for $\Delta 1$ (positive polarity) .....	59
<b>Table 5.2</b> : Test results for $\Delta 2$ (positive polarity) .....	59
<b>Table 5.3</b> : Test results for $\Delta 1$ (negative polarity) .....	60
<b>Table 5.4</b> : Test results for $\Delta 2$ (negative polarity) .....	60
<b>Table 5.5</b> : Trigger pulse magnitude effect for 12 kV trigger pulse, positive polarity and $\Delta 1$ .....	62
<b>Table 5.6</b> : Trigger pulse magnitude effect for 12 kV trigger pulse, negative polarity and $\Delta 1$ .....	62
<b>Table 5.7</b> : Trigger impulse energy analysis, 6 kV trigger pulse, 1 $\mu$ F, positive polarity of impulse voltage generator.....	63
<b>Table 5.8</b> : Trigger impulse energy analysis, 6 kV trigger pulse, 8.2 $\mu$ F, positive polarity of impulse voltage generator.....	64
<b>Table 5.9</b> : Trigger impulse energy analysis, 6 kV trigger pulse, 1 $\mu$ , negative polarity of impulse voltage generator.....	64
<b>Table 5.10</b> : Trigger impulse energy analysis, 6 kV trigger pulse, 8.2 $\mu$ F, negative polarity of impulse voltage generator.....	64
<b>Table 5.11</b> : Unit response parameters of full divider.....	69
<b>Table 5.12</b> : Unit response parameters of half divider. ....	71
<b>Table 6.1</b> : Recommended response parameters for impulse voltage reference measuring systems.....	72



## LIST OF FIGURES

	<u>Page</u>
<b>Figure 1.1</b> : Overall view of an automated IVG. ....	2
<b>Figure 1.2</b> : Whole system of automated IVG . ....	2
<b>Figure 2.1</b> : Classification of overvoltages .....	6
<b>Figure 2.2</b> : Switching impulse. ....	6
<b>Figure 2.3</b> : Standard full lightning impulse.. ....	8
<b>Figure 2.4</b> : Front chopped lightning impulse voltage. ....	9
<b>Figure 2.5</b> : Standard tail chopped lightning-impulse voltage .....	9
<b>Figure 2.6</b> : Basic circuits for impulse generators. ....	13
<b>Figure 2.7</b> : Laplace transform circuit for IVG. ....	14
<b>Figure 2.8</b> : Impulse voltage wave and its components. ....	16
<b>Figure 2.9</b> : Voltage efficiency factor $\eta$ in dependency of capacitance ratio $C_b/C_s$ for lightning impulse $T_1/T_2$ .....	18
<b>Figure 2.10</b> : Multi-stage impulse generator .....	19
<b>Figure 2.11</b> : Earthing in high voltage laboratory .....	22
<b>Figure 2.12</b> : Earthing and shielding of a high-voltage research setup .....	23
<b>Figure 3.1</b> : Basic voltage testing system. ....	30
<b>Figure 3.2</b> : Unit step response setup .....	34
<b>Figure 3.3</b> : Idealized unit step response of an oscillating system with virtual origin .....	35
<b>Figure 3.4</b> : Idealized unit step response of an oscillating system without virtual origin .....	36
<b>Figure 3.5</b> : Multi-stage impulse generator .....	36
<b>Figure 4.1</b> : Typical trigatron system .....	40
<b>Figure 4.2</b> : Two possible way for discharge in trigatron .....	44
<b>Figure 5.1</b> : Impulse voltage generator .....	53
<b>Figure 5.2</b> : The definition of utr parameter. ....	54
<b>Figure 5.3</b> : Side view of trigatron spheres .....	55
<b>Figure 5.4</b> : Front view of trigatron sphere .....	55
<b>Figure 5.5</b> : Trigger impulse generating circuits. ....	56
<b>Figure 5.6</b> : Triggering circuit (as schematic of figure 5.5) .....	57
<b>Figure 5.7</b> : Triggering circuit in connection with the IVG .....	57
<b>Figure 5.8</b> : Trigger pulse wave shape .....	58
<b>Figure 5.9</b> : Comparison of $\Delta 1$ and $\Delta 2$ effect on utr range in presence of trigatron and positive polarity of the generator .....	60
<b>Figure 5.10</b> : Comparison of $\Delta 1$ and $\Delta 2$ effect on utr range in presence of trigatron and negative polarity of the generator .....	61
<b>Figure 5.11</b> : Comparison of trigger pulse voltage magnitude for 6 and 12 kV trigger pulse with $\Delta 1$ and positive polarity of generator. ....	63
<b>Figure 5.12</b> : Comparison of trigger pulse energy effect on utr for, 6 kV trigger pulse, positive polarity .....	65

<b>Figure 5.13</b> : Comparison of trigger pulse energy effect on utr for, 6 kV trigger pulse, negative polarity .....	65
<b>Figure 5.14</b> : Unit step response setup .....	66
<b>Figure 5.15</b> : Applied unit step pulse waveform .....	67
<b>Figure 5.16</b> : Unit step response of full divider, $R_d = 0$ , Rise time = 58 ns .....	68
<b>Figure 5.17</b> : Unit step response of full divider, $R_d = 100 \Omega$ , Rise time = 159 ns ...	68
<b>Figure 5.18</b> : Unit step response of full divider, $R_d = 280 \Omega$ , Rise time = 658 ns ...	69
<b>Figure 5.19</b> : Unit step response of half divider, $R_d = 0 \Omega$ , Rise time = 85 ns.....	70
<b>Figure 5.20</b> : Unit step response of half divider, $R_d = 100 \Omega$ , Rise time = 347 ns...	70
<b>Figure 5.21</b> : Unit step response of half divider, $R_d = 280 \Omega$ , Rise time = 992 ns...	71

# **AN AUTOMATION OF HIGH VOLTAGE IMPULSE GENERATOR**

## **SUMMARY**

An uninterrupted supply of electricity is of supreme importance in all our activities. Transient over-voltages and over-currents due to lightning and switching surges are the main causes of interruption of the continuous supply of electricity by causing a breakdown of insulation of the transmission lines and various power apparatus thus causing severe damage to these equipments. So power apparatuses are generally required to undergo several insulation tests to demonstrate that the equipment fulfills the specified requirements and quality standards. High voltage laboratories are an essential requirement for making acceptance tests for equipments that go into operation in the high voltage transmission systems.

Istanbul Technical University, Fuat Kulunk High Voltage Laboratory is the biggest high voltage laboratories in Turkey that performs high voltage tests for industrial utilities and academic researchers. The laboratory consists of several blokes that perform various tests. The one MV six stages impulse voltage generator (IVG) that is located in B block can perform lightning impulse tests with a range of 10 kJ output.

The mentioned IVG that is the case of study for this thesis supposed to have more accurate output and flexible control for the operator during the tests. To make it possible, we propose an overall view of an automated generator, which includes a computer aided system to control, record and analysis the whole system. The hardware required for such a system demands some additional parts for generator itself to have more its output voltage as desired for the test properties, while it is even within national and international standards. Since computerized part of proposed system postponed for as future job and is not included in this thesis study, we will go with the other parts.

Typical IVGs are consisted of some stages with capacitors and resistors that work in series connection via spark gaps. It is the main structure of any IVG in high voltage laboratories. The generated impulse wave shape is a function of some parameters from generator structure (elements of generator such as capacitors, resistors, inductances, sphere gaps and ...) and some environmental conditions (such as dirt and humidity of air, pressure).

In this study, most interested parameters are those affecting the magnitude of output impulse. For known generator elements that satisfy standard wave shape, in a constant DC charging voltage, the distance between sphere gaps of stages influences the magnitude of the output voltage. It means that with no additional tool obtaining the desired magnitude for produced impulse will be hard and somehow impossible. For this reason, to have a precise magnitude, a system called trigatron installed on the generator that makes it able to generate any impulse voltage with desired magnitude. During some tests, the behavior of the generator in presence of the

trigatron analyzed and more details are mention that it leads to a more accurate output.

A voltage divider that can operate in one MV (full mode) and 0.5 MV (half mode) range have used to measure the output signal of the one MV six stages impulse generator. An impulse voltage has generated in some KVs and must lower to scales of some volts to be monitored. It is important to obtain the impulse voltage as proper scale of that to be demonstrated on oscilloscope or a digital recorder. During the connections between generator and divider and divider to monitoring tools, some disturbances can be imposed on the impulse wave shape and make it unfit the standards. To analysis the accuracy of measuring system, a unit step response of the divider is evaluated. For this reason, a step pulse generator is established according to international standards. The results are used to define some parameters of the divider in both full and half mode.

## YÜKSEK DARBE GERİLİMİ ÜRETİCİNİN OTOMASYONU

### ÖZET

Günümüzde kullanılan güç sistemlerinin büyük kapasitede olmalarıyla beraber, hassas olmaları da gerekmektedir. Güç sisteminde kullanılan bir elemanın arızalanması sistemin büyük bir kısmının devre dışı kalmasına ve güvenilirliğinin ve performansının azalmasına sebep olur. Bu arızalar genellikle elektrik cihazların yalıtım kısımlarında ortaya çıkan bozulmalarla bağlantılıdır. Özellikle yüksek gerilim cihazları, sürekli olarak şebeke gerilimleri ve aşırı gerilimlerle zorlandıkları için, daha da çok yalıtım bozulmalarına maruz kalabilirler. Şebekede oluşan aşırı gerilimler şebeke kaynaklı (anahtarlama olayları) olabildiği gibi ve şebeke dışından da yıldırım düşmesi sonucu aşırı gerilimler oluşabilir. Anlatılan nedenlerden dolayı yüksek gerilim cihazlarının yalıtımlarının aşırı ve sürekli gerilimlere dayanıklılıkları belirlenmelidir. Söz konusu olan incelemeler yüksek gerilim laboratuvarlarında yapılmaktadır.

Sanayi sektöründe faaliyet gösteren üreticiler, üretmiş oldukları ürünleri ilgili ulusal, uluslararası ve çeşitli askeri standartlara göre test ettirmelidirler. Bu testler, kendi bünyelerinde bulunan laboratuvarlarda veya uluslararası geçerliliği olan akredite olmuş laboratuvarlarda gerçekleştirilmelidir. Testler sırasında kullanılan test aletlerinin kalibre olması ve standartlara uyması gerekmektedir.

Yüksek gerilim mühendisliğinde olan ilerlemeler cihazların daha da hassas ve net incelenmelerini talep etmektedir. Bu yüzden yüksek gerilim laboratuvarlarında yapılan deneyler her zaman yenilikçi ve uluslararası standartlara uygun olmalıdır. İstanbul Teknik Üniversitesi'nde bulunan Fuat Külünk Yüksek Gerilim Laboratuvarı Türkiye'nin en büyük yüksek gerilim laboratuvarıdır. Bu laboratuvarda hem bilimsel araştırmalar hem de endüstriyel deneyler gerçekleştirilmektedir. 4000 m<sup>2</sup>'lik bir alan üzerinde kurulmuş olan bu laboratuvar A, B ve C olarak adlandırılan üç bloktan oluşmaktadır. Tez konusu olan 6 katlı 1 MV'luk Darbe Gerilimi Üretici laboratuvarın A blokunda yer almaktadır.

Darbe gerilimi üreteçlerinin esas yapısı kondansatör ve dirençlerden oluşan (darbe şeklini değiştirmek amacıyla endüktanslar da olabilir) katların küresel elektrotlar üzerinden seri bağlantılarından oluşur. Darbe üretici devresindeki dirençler, kondansatörler, küresel elektrot açıklıkları çıkış geriliminin tepe, cephe ve sırt değerlerini belirlemektedir. Uluslararası standartlara uygun bir darbe gerilimi üretebilmek için darbe gerilimi üreteç devresindeki elemanların belirli değerlerde olmaları gerekmektedir. Üretilen darbenin şekline etkisi olan parametrelerin dışında, havadaki nem ve kir, hava basıncı ve sıcaklık gibi parametrelerin etkisi de göz önüne alınmalıdır. Tezde esas parametre olarak incelenen konu, katlar arasındaki kürelerin aralıklarıdır. Bu aralıklar darbe geriliminin genliğini değiştirmektedir. Belirli bir darbe gerilimi üretici için sabit bir DC giriş geriliminde, küre aralıklarındaki değişim, üretilen darbe geriliminin genliğini değiştirecektir. Ancak istenen darbe genliğini elde etmek için küre aralığını değiştirmek her zaman istenilen genliğin elde edilmesini sağlamayabilir. Küre meafelerinin ayarlayan elektromekanik cihazlar ne kadar hassas

yapısalarda, küre aralıklarında ufak bir değişimle çıkışta büyük bir değişim oluşacaktır. Bu yüzden darbe gerilimi üretici için daha esnek bir çalışma sağlamak ve istenen genlikte darbe gerilimi elde etmek için bir tetikleme sistemi tasarlanmıştır. Tetikleme sistemi farklı darbe üreteçleri için kullanılabilir ve çıkış darbenin tamamen küre aralıklarındaki değişime bağlı olmamasını sağlar. Başka bir deyişle belli bir genliğe kadar küre aralıklarının değişimi ile ayar yapılır ve tam genliği elde etmek için tetikleme sistemi kullanılır. Tetikleme sistemleri genel olarak aynı prensiplere sahip olurlar.

Bu tezde kullanılana tetikleme sistemi bir darbe işaretinin uygulanmasını esas alarak tasarlanmıştır. Başka bir devre üzerinden bir darbe gerilimi üretildikten sonra, bu darbe yüksek gerilim kablosuyla belirli bir küreye uygulanır ve istenen anda darbe gerilimi üretecin çıkışına uygulanır. Uygulanan darbe işareti çıkış darbenin parametrelerini değiştirmemektedir ve ancak küreler arasındaki atlamayı sağlamaktadır. Darbeyi üreten devrede 220 voltluk ac gerilim bir trafo üzerinden 150 voltluk dc bir gerilime çeviriliyor. Üretilen dc gerilim yüksek voltlu bir direnç üzerinden bir kondansatörü doldurmaktadır. Kondansatör dolduktan sonra başka bir direnç üzerinden tristör vasıtasıyla yüksek gerilim trafosunun giriş tarafına (primary) uygulanmaktadır. Yüksek gerilim trafosunun diğer ucu topraklanmıştır (giriş tarafında). Tristörün ateşlenmesi için 220/12 voltluk bir trafo kullanılarak bir anahtar üzerinden 12 voltluk dc gerilim tristörün gate ucuna uygulanmıştır. Tristörün anahtarlandığı zaman kondansatör direnç üzerinden boşalarak yüksek gerilim trafosunun çıkış tarafında 6 kV luk bir gerilim üretilmektedir. Üretilen darbe gerilimi yüksek gerilim kablosuyla darbe gerilimi üretecin birinci katında bulunan küreye uygulanmaktadır. Darbe gerilimi birinci küreye uygulandıktan sonra birinci katda atlama başlayıp ve bu atlama diğer katlarda da tekrarlanacaktır. Birinci trafonun giriş gerilimine göre yüksek gerilim trafosunun çıkışı farklı değerlere sahip olabilir. Üretilen darbe işaretin genliği, sistemin tetiklenmesindeki etkisini incelemek için, dc gerilim değiştirerek 6kV luk ve 12 kV luk darbe işaretleri uygulanmıştır.

Trigatron olarak bilinen sistemin tasarlanmasında, farklı deneyler için istenen özelliklere sahip darbe gerilimi elde edilecektir. Trigatron'un etkisi üreticinin pozitif ve negatif polaritelerinde farklı deney gerilimleri altında incelenmiştir. Trigatron sistemi için yeni bir parametre ( $u_{tr}$ ) tanımlanmıştır ve bu parametrenin küre açıklığıyla bağlantısı incelenmiştir. Söz konusu olan parametre incelenen darbe gerilimi üretici ile pratikte yapılan deneyler için kullanılabilir.

Trigatron sistemi bir tristör üzerinden darbe üreticinin birinci katında bulunan küreye 6 kV'luk bir darbe gerilimi uygulamakta ve böylelikle diğer kürelerde de atlama olmasını sağlamaktadır. Bu 6 kV'luk darbe gerilimi katlardaki kondansatör geriliminin istenildiği değerinde uygulanabilir. Dolayısıyla üretilen darbe geriliminin genliği istenilen değere ayarlanabilmektedir. Ancak, belirli bir küre açıklığında, belirli bir doğru gerilim için tüm kürelerde atlama olması sağlanmalıdır (tetikleme sistemi için önerilen parametrenin genliği). Bu parametre çıkış darbe geriliminin genliğini istediğimiz değerde sağlanması demektir. Utr parametresine ne kadar büyük ise , sabit bir küre aralığında farklı darbe genlikleri elde etmesi kolay olacaktır.

Tetiklenen kürenin, tetikleme işaretini küreye bağlayan kablonun ve diğer yalıtımlı olan cihazlar ve bağlantıların belirli bir gerilime kadar dayanıklıdır. Ayrıca daha güçlü ve büyük darbe işaretleri üretmek için, tetikleme sisteminde olan elemanların daha büyük bir değerlere sahip olmaları gerekmektedir. Bu yüzden tetikleme işaretinin genliği ve gücünün etkisi incelenmiştir. Deneyler sonucuyla elde edilen



sonuçlara göre, tetikleme işaretinin genliği ve gücü belli bir değerden sonra tetiklemede etkisi olmadığı görünmüştür. Bu nedenle tetikleme sisteminde olan elemanların daha az zorlanması için gereken değerler (genlik ve güç) alınmalıdır. Bu değerler birinci trafonun dc çıkışı (kondansatörü dolduran gerilim) ve kondansatörün değerleri ile belirlenmektedir.

Tetikleme sistemi hazır olduktan sonra darbe üreteğine bağlanmıştır. Belirli bir genlikte olan darbe gerilimini elde etmek için sabit bir küre aralığında darbe üreteçinin giriş gerilimi basamaklı olarak artırmaktadır, istenilen genlikte tetikleme anahtarını basarak sistem tetiklenmiş olacaktır. Böylece farklı deneyler için istenilen darbe genliği uygulama imkanı olacaktır.

Tetikleme sisteminin olmadığında, darbe gerilimi üreteçinin çıkışını istenilen genlikte darbe üretebilmesi için küre aralıklarının değiştirilmesi gerekmektedir. Bu değişimler elektromekanik elemanları aracılığıyla yapıldığına göre, her ayarlama aynı küre aralığına ulaşılmadığı için aynı darbe gerilimlerini elde etmek zor olacaktır.

Bu tez çalışmasında daha etkin bir tetikleme sisteminin tasarlanması için önerilen tetikleme sisteminin fiziksel çalışma mekanizması, ilgili matematiksel eşitlikler ile açıklanmıştır. Deneyler sonucunda tetikleme darbe geriliminin genliği ve enerjisinin utr parametresinin genliğine etkisi olmadığı görülmüştür.

Üretilen darbe geriliminin genliğinin ölçülebilmesi ve şeklinin incelenebilmesi için gerilim bölücüler kullanılır. Darbe gerilimi şeklinde, gerilim bölücü ile ölçü sistemi arasındaki bağlantılar ve bölücünün kendi yapısından kaynaklanan, bir takım parazitler olabilir. Bu etkenler sonucunda çıkış darbe geriliminin şekli değişmiş olabilir ve bazı aşımalar ortaya çıkabilir. Bu aşımalar genelde üretilen darbe geriliminin sırt ve cebhesinde yer almaktadırlar. Bu yüzden İTÜ yüksek gerilim laboratuvarında bulunan gerilim bölücünün parametreleri incelenmiştir.

Bu çalışmada, gerilim bölücünün üretilen darbe geriliminin şekline etkisini inceleyebilmek için, bölücünün birim basamak cevabı (unit step response) incelenmiştir. Bu inceleme uluslararası önerilen standartlarla uygun bir düzenle yapılmıştır. Birim basamak gerilimi üreten bir devre ile yükselme zamanı 33 ns ve doğru gerilim genliği 158 volt olan bir basamak fonksiyonu elde edilmiştir. Birim basamak fonksiyonunu üretmek için civa rölesi kullanılmıştır. Birim basamak üreticinin çıkışı bir sönmüleme direnci üzerinden gerilim bölücünün yüksek gerilim girişine uygulanmıştır. Birim basamak fonksiyonunu uygulamak için tüm bağlantılar levha şeklinde olan bakır bağlantılardan oluşmuştur. Bu bağlantılar kablunun kendisinden oluşabilen elektromanyetik yüklenmeleri önlemektedir.

Uygulanan birim basamak geriliminin cevabı, gerilim bölücünün alçak gerilim tarafından bir 200 MHz'lik osiloskop yardımı ile incelenmiştir. Kullanılan osiloskop bilgisayara bağlanarak Lab View programı üzerinden kontrol edilebilmektedir. Tüm cevaplar program tarafından bir Excell dosyasında kaydedilmektedir. Dolayısıyla üretilen darbe şekli zaman eksenine ve genlik eksenine göre sayılarla elde edilmiştir. Bu veriler birim basamak fonksiyonunun parametrelerini hesaplamak için kullanılmıştır. Mathlab de bir .m programı hazırlandıktan sonra bu parametreler hesaplanmıştır. Bu incelemede 1 MV'luk gerilim bölücünün 1 MV ve 0,5 MV'luk ölçme konumları için çevirme oranları elde edilmiştir. Elde edilen sonuçlar bir gerilim bölücü için uluslararası standartların belirlediği parametreleri sağladığı görünmektedir.

Sonu olarak tetikleme sisteminin darbe gerilimi retelerde olması daha standart deneyler yapılmasını saėlamaktadır. Tetikleme sistemi var olan darbe gerilimi reteinde daha esnek bir kumanda olanaėı olduėundan, operatr (deneyleri yapan teknik elemanlar) uluslar arası kabullenmiř standartlara uygun deneylerin yapılmasını saėlıyabilmektedirler. İT yksek gerilim laboratuvarında yer alan 6 katlı yksek darbe gerilim reteinin tetikleme sistemi eklendikten sonra, deneyler sırasında kolaylıksaėladıėı grnmektedir. Ayrıca lm iin kullanılan gerilim blcnn de parametreleri doėru bir lm saėladıėı grnmektedir.

## **1. INTRODUCTION**

An uninterrupted supply of electricity is of supreme importance in all our activities. Transient over-voltages and over currents due to lightning and switching surges are the main causes of interruption of the continuous supply of electricity by causing a breakdown of insulation of the transmission lines and various power apparatus thus causing severe damage to these equipments. So power apparatuses are generally required to undergo several insulation tests to demonstrate that the equipment fulfills the specified requirements and quality standards. High voltage laboratories are an essential requirement for making acceptance tests for the equipment that go into operation in the high voltage transmission systems.

The impulse generator is designed to produce two impulse voltages, the lightning and the switching impulses. There is a increasing demand for more accurate test which means impulse voltages generation, measurement and analysis must be carried out with a high accuracy. Nowadays preferred high voltage laboratories are those equipped with flexible and precise test tools. Impulse voltage generators have a remarkable role in this category. Being capable of these demands they must be updated too.

Fuat Kulunk high voltage laboratory of ITU (Istanbul Technical University) is the biggest high voltage laboratory Turkey. The subject of this thesis is to automate 1 MV six stages Impulse Voltage Generator (IVG) in this laboratory which is expected to lead the generator to more flexible and accurate operation.

The overall view of an automated IVG is shown in figure 1.1. The aim of this thesis is to some parts of this view, including trigatron system and precise measuring of generated impulse voltage and the computer aided part remains as future job.

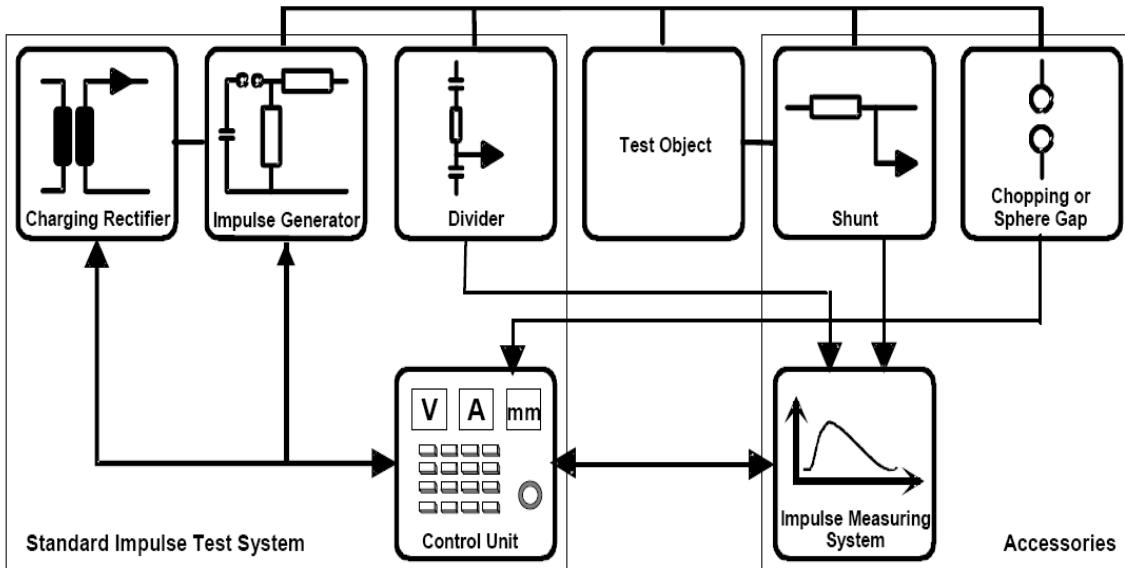


**Figure 1.1:** Overall view of an automated IVG [8]

Depending on type of the IVG some of the block diagrams may not exist. For example “chopping or sphere Gap” is for generators capable of generation chopped impulses. The IVG under study in ITU is used for generate standard impulse voltages.

The proposed hardware supporting this block diagram configuration is like figure 1.2 that includes all done parts by the thesis. For now only computer controlled part is not added to the study.

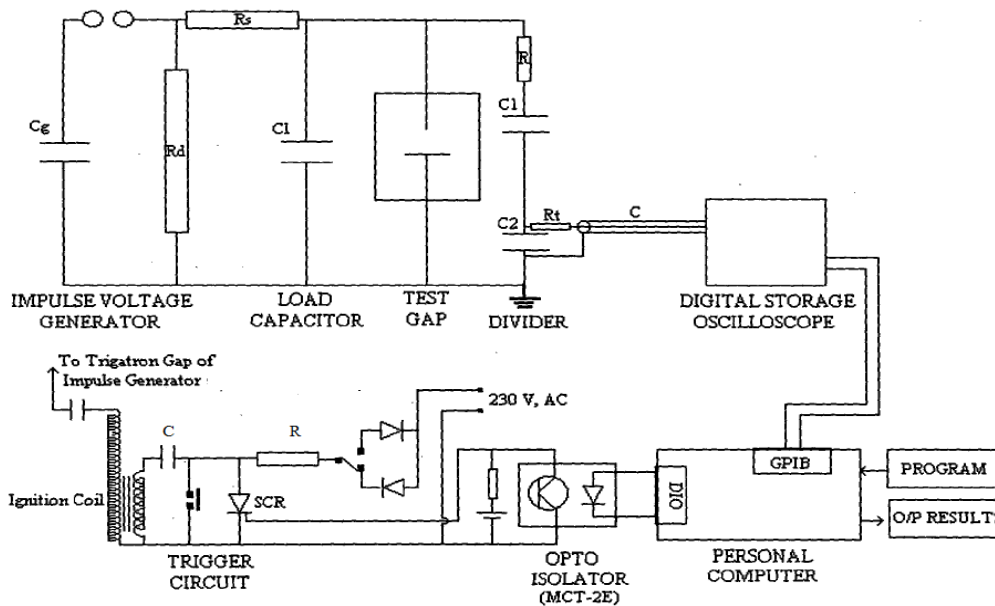


**Figure 1.2:** Whole system of automated IVG [21]

The oscilloscope used to see output waveforms is a 200 MHz one which is in control room.

In the proceeding chapters, in chapter two the possible overvoltages than can occur in a power system will be discussed in details and it will be seen that they can be categorized in two groups:

- External overvoltages
- Internal overvoltages

For each category some the international standard definitions will be clarified. In chapter three standard lightning and switching impulses will be discussed in detail. Since to generate these impulse voltages in desired form needs more details of their properties, mathematical formulation of them is brought out.

One of the important parts of the high voltage engineering is measurement of generated waveforms. Since impulse voltages have a very fast rise time, the measuring system must be capable of sensing these fast impulses. On the other hand the connections between IVG and the measuring system, and even electromagnetic environment can impose disturbances to the generated impulses. Chapter four deals with impulse voltage measurement.

In chapter five, the definitions and mechanism of trigatron system will be discussed. The history and the fundamental aspects of trigatron can make it easier to understand how it works in an IVG.

In chapter six, the practical results of diagram of figure 1.2 is presented. After installing the trigatron system on the generator, during some test, the parameters that can affect the system performance are denoted. A parameter,  $u_{tr}$ , which it's widths has a relationship with flexible operation of IVG is introduced. For both positive and negative polarities of generator the trigatron system is tested and the results are compared.

To evaluate the performance of the voltage divider used with the 1 MV impulse generator, the evaluation of unit step response is applied for both full and half divider positions. From this analysis the divider ratio is calculated.



## **2. IMPULSE VOLTAGES GENERATION and TESTS**

### **2.1 Overvoltages in Power Systems**

Overvoltages in the power system can be classified into two categories:

- External overvoltages
- Internal overvoltages

External over-voltages have their origins on atmospheric perturbation. The most important of them are the lightning flashes.

Internally generated overvoltages are mostly from switching operations in the system such as switching of capacitive and electromagnetic loads and travelling waves due to the energizing of transmission lines. Also taken into consideration are power frequency overvoltages, which are caused either by load rejection or by voltage changes on the two healthy phases when a single-phase fault occurs.

Power frequency voltages are important since they affect the rating of protective arresters or coordinating gaps that provide a means of controlling the overvoltages for the purpose of insulation co-ordination.

As a classification for what mentioned above, overvoltages that must be taken in account for insulation coordination in a power systems, there can be four types of over-voltages in a system:

1. Power frequency voltage under normal operating conditions
2. Temporary overvoltages
3. Switching overvoltages
4. Lightning overvoltages [4]

Figure 2.1 shows this classification on a curve description.

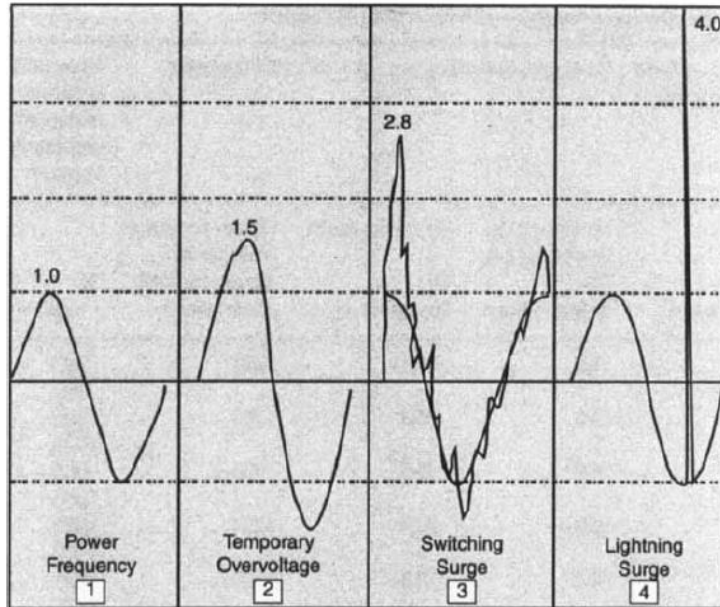


**Figure 2.1:** Classification of overvoltages [1]

### 2.1.1 Standard switching impulse voltage

For test purposes, switching voltages have standard wave shape as defined in national and international standards. In IEC-60060-1 standard, the switching impulse voltages and its parameters are defined in figure 2.2.

Switching-impulse voltage is an impulse voltage with a front time of 20  $\mu$ s or longer. Figure 2.2 shows a switching impulse with parameters.

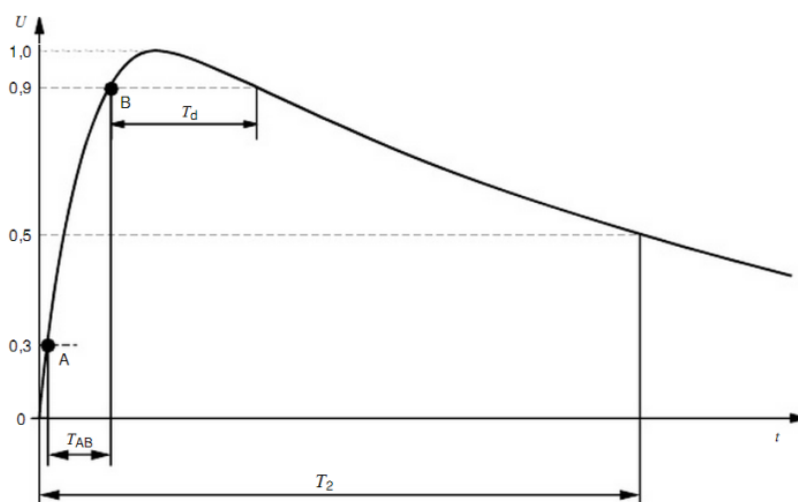


**Figure 2.2:** Switching impulse voltage (IEC 2218/10).



Where in the figure 2.2:

O: true origin (Instant where the recorded curve begins a monotonic increase (or decrease))

$T_2$ : time to half-value (Time interval between the true origin and the instant when the voltage has first decreased to half the maximum value)

$T_d$ : time above 90 % (Time interval during which the switching-impulse voltage exceeds 90 % of its maximum value)

$T_p$ : time to peak (Time interval from the true origin to the time of maximum value of a switching-impulse voltage)

The standard switching-impulse voltage is an impulse having a time to peak  $T_p$  of 250  $\mu\text{s}$  and a time to half-value  $T_2$  of 2500  $\mu\text{s}$ . It is described as a 250/2500 impulse.

Permitted tolerances for switching impulses:

- a) Wave time to peak:  $250 \pm 50 \mu\text{s}$
- b) Wave time to half-value:  $2500 \pm 1500 \mu\text{s}$
- c) Wave peak value:  $\pm 3\%$  of required magnitude

### 2.1.2 Standard lightning impulse voltage

Lightning flash can be presented with various wave shapes and parameters, but for test aims standards defines are available. Here is what brought in IEC-60060-1. Figure 2.3 shows a standard Full lightning impulse voltage and time parameters.

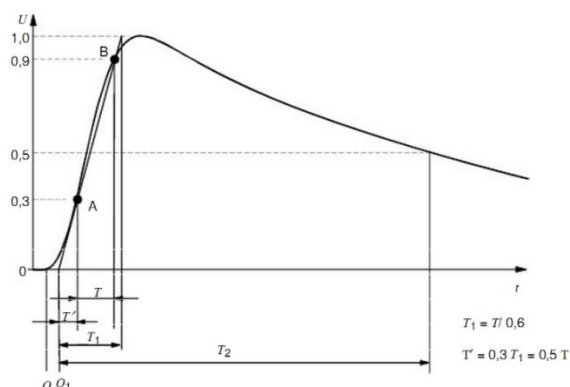


**Figure 2.3:** Standard full lightning impulse voltage (IEC 2211/10).

In the figure above:

$T_1$ : front time

Virtual parameter defined as  $1/0,6$  times the interval  $T$  between the instants when the impulse is 30 % and 90 % of the peak value on the test voltage curve (points A and B, Figure 2.3). Standard time for this interval is  $1.2 \mu\text{s}$ .

$O_1$ : virtual origin (Instant preceding that corresponding to point A, of the test voltage curve by a time  $0,3T_1$ )

$T_2$ : time to half-value

Virtual parameter defined as the time interval between the virtual origin,  $O_1$ , and the instant when the test voltage curve has decreased to half the test voltage value. The standard time for this interval is  $50 \mu\text{s}$ .

### 2.1.3 Front chopped lightning-impulse voltage

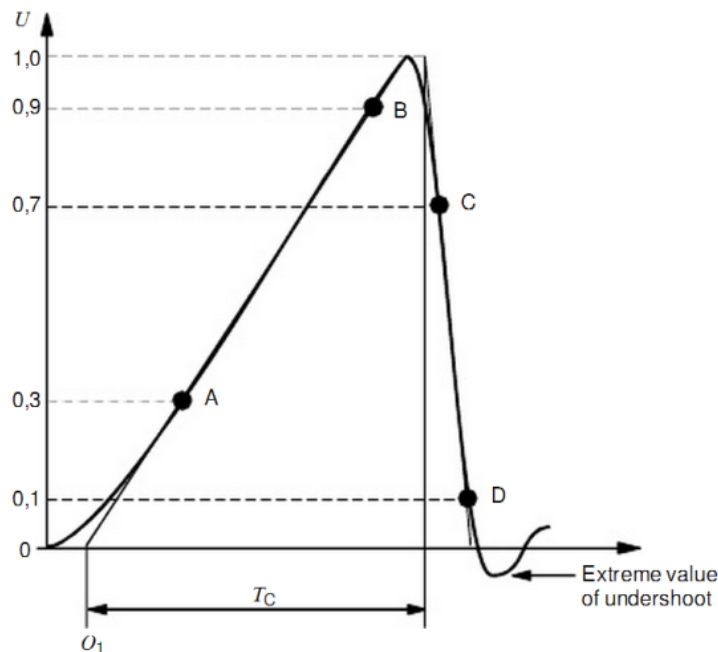


**Figure 2.4:** Front chopped lightning impulse voltage (IEC2214/10)

Virtual parameter defined as the time interval between the virtual origin  $O_1$  and the instant of chopping.

### 2.1.4 Tail Chopped Lightning Impulse Voltage

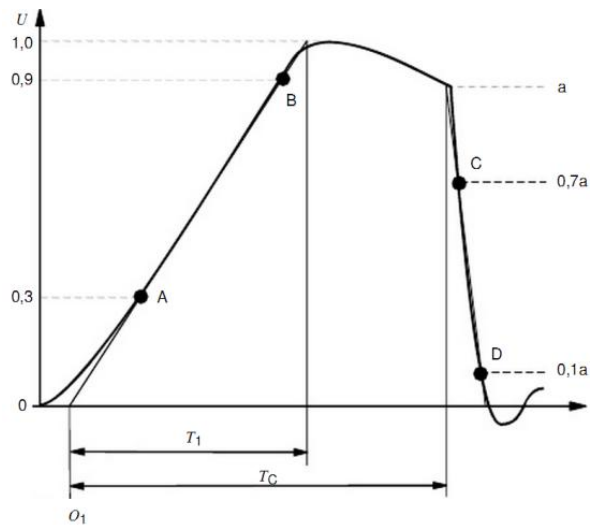


**Figure 2.5:** Standard tail chopped lightning-impulse voltage (IEC 2215/10).

Because of difficulty in obtaining the exact time intervals, IEC permits a tolerance for the standard wave shape.

A wave within the following tolerances shall be used for lightning impulses:

- a) Wave front time:  $1.2 \pm 0.36 \mu\text{s}$
- b) Wave time to half-value:  $50 \pm 10 \mu\text{s}$
- c) Wave peak value:  $\pm 3\%$  of required magnitude

### 2.2 Overvoltages Effect on Power System

On the path from generation of electricity to its use by costumers, many components in between take care of the transmission and distribution of the electrical energy. All of these have insulation design aspects. System voltages and currents, as well as overvoltages and short-circuit currents expected, are important parameters in designing power system networks. These also influence what possible insulation to use. For example, most transmission lines all across the world are overhead lines, whereas for the distribution level cable networks for distribution of electrical energy can serve many urban areas. In a running power system at any time, there may be internal or external overvoltages. The most effected part of electrical system during any type of overvoltages is the insulation of the equipments. All insulating materials

fail at some level of applied voltage, and ‘dielectric strength’ is the voltage a material can withstand before breakdown occurs. Table 2.1 shows dielectric strength of some insulating materials.

**Table 2.1:** Dielectric strength of some materials [3]

Material	Dielectric Strength (MV/m)
Air	3
Amber	100
Glass	17
Porcelain	10
Polystyrene	24
Oil	10
Mica	100
Bakelite	24
Cellulose paper	10
Perspex	40
Barium titanate	5

When the period that equipment is under overvoltage is long and when the magnitude of that is greater than the withstanding strength of insulating material, it breaks down and causes failure in that equipment and then the system fails. Depending on the role of the failed element, some parts of the power system can be outaged. Therefore specifying the insulating strength, which is known as insulation coordination, will be necessary. In simple definition, insulation coordination is the selection of the strength of the insulation. “ Insulation Coordination is defined as selection of dielectric strength of equipment in relation to the operating voltages and overvoltages which can appear on the system for which the equipment is intended and taking into account the service environment and the characteristics of the available preventing and protective devices ( As per IEC 60071). The selection of insulation strength consistent with expected over-voltages to obtain an acceptable risk of failure (As per IEEE 1313.1).

Overvoltages are compared to insulation strength to obtain a value for protective margin. Before making this comparison, it may be necessary to adjust the standard insulation strength provided for equipment to account for (1) nonstandard wave shapes of overvoltages and/or (2) nonstandard atmospheric conditions. There are several methods of describing the strength, such as the BIL, BSL, and CFO, which must be defined.

### **2.3 High Voltage Tests**

The study of insulation coordination has generated an inventory of overvoltages as well as survey of mechanisms that endanger the H.V. components at operating voltage. It shall be ascertained that the components will withstand these dangers for a lifetime of 30 to 50 years.

For this reason, tests have been devised which are defined in test specifications. These specifications describe tests for lightning and switching impulses, AC voltage and DC voltage, combined with heat cycles, load cycles, mechanical loads, etc. in addition, outdoor equipment is subjected to environmental tests such as rain tests, pollution tests, climate tests, etc.

If a component satisfies all these tests, there is a fair chance that it will perform well in operational circumstances. Most specifications comprise four categories of tests:

- Type tests
- Sample tests
- Routine tests
- Tests after installation

Type tests are performed once on a newly designed component, to establish that this design will perform well in service. The type test is not repeated unless essential modifications in the design have been made, such as the use of other materials, an increase in the sign stress, a change in the configuration, etc.

Sample tests are performed on samples that are chosen at random from a number of components that are to be supplied; one voltage transformer out of 200 transformers, or one sample of 10 m cable out of 10 km of cable for instance. Sample tests are performed to check whether a batch of products is of the agreed quality. As in the type test, these tests are destructive and the sample is not supplied to a user after the test. Routine tests are tests performed on all items to be supplied. They are non-destructive tests [6].

Tests after installation are supplementary to routine tests: in some cases, a component is installed on site, for instance, a large power transformer, which was too

large to be shipped in one piece; or a circuit of an underground power cable. The test is performed to check whether the installed product is fit for use.

Test specifications are based on a standard operating voltage as discussed. In subsequent sections, examples of test specification are discussed: two components for AC networks and a cable for DC transmission.

In the above cases, only overvoltage tests are discussed. Test specifications contain a multitude of mechanical tests, materials test, checks on the construction, etc. that ignored here [6].

**2.4 Impulse Voltage Generating Circuits**

Impulse voltage tests are used to determine possible lightning attachment points and breakdown paths across or through non-conducting materials. To generate standard lightning and switching impulses, generally high voltage generators are used in laboratories. The two basic circuits for impulse generators are shown in Figure 2.6.

In the figure 2.6  $C_s$  is impulse capacitor,  $R_d$  is damping resistor,  $R_e$  is discharge resistor and  $C_b$  is load capacitor. The two basic circuits of Figure 3.1 differ only in the positioning of the discharge resistor  $R_e$ . In circuit “a”, the resistors  $R_d$  and  $R_e$  form a voltage-dividing system.

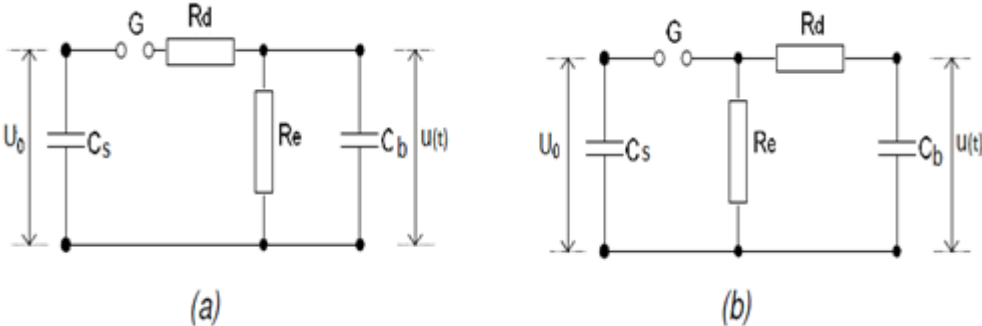


**Figure 2.6:** Basic circuits for impulse generators

The mechanism that the circuit runs is simply charging and discharging of load capacitance  $C_b$ . Initially, the impulse capacitor  $C_s$  charges slowly from a dc voltage source (charging-rectifier) up to the charging voltage  $U_0$ . Then impulse capacitor  $C_s$  discharges on  $C_b$  through damping resistor  $R_d$  via switching gap of  $G$ . This spark gap acts as a voltage-limiting and voltage-sensitive switch [3]. The elements of the generator will shape the curve of output voltage.  $R_d$  will primarily damp the circuit

and control the front time  $T_1$ .  $R_e$  will discharge the capacitors and therefore essentially control the wave tail.

In the standard impulse voltage, the time to front is short and time to tail is longer than that. It means rapid charge and slow discharge of load capacitor  $C_b$  to the peak value. To achieve that, we need to set  $R_e \gg R_d$ . thus the value of  $R_d C_s$  determines the time that  $u(t)$  reaches to its peak value. A big value leads to a smaller time to peak. Time to tail is controlled by time constant  $C_s (R_d + R_e)$  for circuit (a), and  $C_s R_e$  for circuit (b).

The main characteristic data for the impulse voltage generator are the charging voltage  $U_0$ , the energy  $W$  stored in the surge capacitor  $C_s$  and the voltage efficiency  $\eta$ . The stored energy is given by:

$$W = \frac{1}{2} C_s U_0^2 \quad (2.1)$$

The peak value, that load capacitor  $C_b$  can be charged is  $U_p$ .  $U_p$  is always smaller than  $U_0$ . Voltage efficiency for generator is given by equation below:

$$\eta = \frac{U_p}{U_0} = \frac{C_s}{C_s + C_b} \quad (2.2)$$

Because of higher efficiency factor of circuit (b), impulse generators are mostly built with that connection.

Design of impulse generator needs to define proper relationships between value of circuit elements ( $C_s$ ,  $C_b$ ,  $R_d$ , and  $R_e$ ) and characteristics of output voltage shape (impulse voltage). When switch gap of G is ignited, it can be assumed as a short circuit. For the analysis, we use the Laplace transform circuit. Figure 2.7 shows that circuit.

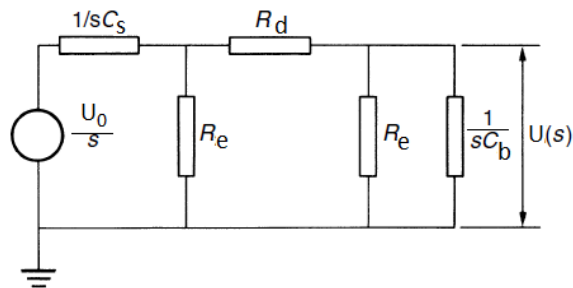


**Figure 2.7:** Laplace transforms circuit for IVG.

In the transform circuit as the boundary condition, for  $t \leq 0$   $C_s$  is charged to  $U_0$  and for  $t > 0$  this capacitor is directly connected to the wave shaping network (connection of  $R_d$ ,  $R_e$ ,  $C_b$ ). For the circuit (a) the output voltage is thus given by the expression:

$$U(s) = \frac{U_0}{S} \frac{Z_2}{Z_1 + Z_2} \quad (2.3)$$

Where:

$$Z_1 = \frac{1}{C_s S} + R_d \quad (2.4)$$

$$Z_2 = \frac{R_2/C_b S}{R_e + 1/C_b S} \quad (2.5)$$

By substitution we find

$$U(s) = \frac{U_0}{k} \frac{1}{S^2 + aS + b} \quad (2.6)$$

And in (2.6)

$$a = \frac{1}{C_s R_d} + \frac{1}{C_b R_d} + \frac{1}{R_e C_b} \quad (2.7)$$

$$b = \frac{1}{C_s C_b R_e R_d} \quad (2.8)$$

$$K = C_b R_d \quad (2.9)$$

For circuit (b) from Laplace transform circuit we have the same general expression in (2.3) and the constants are as following:

$$a = \frac{1}{C_s R_d} + \frac{1}{C_b R_d} + \frac{1}{R_e C_s} \quad (2.10)$$

$$b = \frac{1}{C_s C_b R_e R_d} \quad (2.11)$$

$$K = C_b R_d \quad (2.12)$$

Constants  $b$  and  $k$  in both circuit connections of (a) and (b) are same.

By solving the Laplace equations that mentioned above in time domain, we obtain:



$$u(t) = \frac{U_0}{k} \frac{1}{(\alpha_2 - \alpha_1)} [\exp(-\alpha_1 t) - \exp(-\alpha_2 t)] \quad (2.13)$$

Where  $\alpha_1$  and  $\alpha_2$  are the roots of the equation  $S^2 + aS + b = 0$ , or

$$\alpha_1, \alpha_2 = \frac{a}{2} \pm \sqrt{\left(\frac{a}{2}\right)^2 - b} \quad (2.14)$$

The output voltage  $u(t)$  is therefore the superposition of two exponential functions of different signs. According to (2.14), the negative root leads to a larger time constant  $1/\alpha_1$  than the positive one, which is  $1/\alpha_2$ . A graph of the (2.13) is shown in Figure 2.8 and a comparison with Figure 2.7 demonstrates the possibility to generate both types of impulse voltages with these circuits.

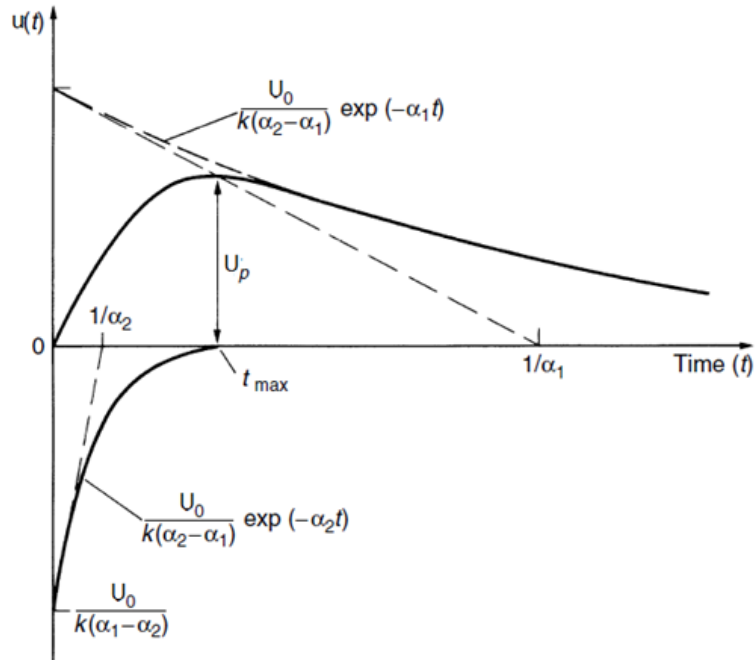


**Figure 2.8:** The IV wave and its components according to circuit in figure 2.1.

To compare circuit (a) and (b) we calculate the voltage efficiency factor for both circuits.

As defined before voltage efficiency for impulse generator is as below:

$$\eta = \frac{U_p}{U_0} \quad (2.15)$$

Where  $U_0$  is the value of dc source that charges impulse capacitor  $C_s$  and  $U_p$  is the maximum value that load capacitor  $C_b$  can reach. From (2.3) it can be seen that  $U_p$  occurs at  $t_{\max}$ . By calculating  $t_{\max}$  from  $\frac{du(t)}{dt} = 0$  we have:

$$t_{\max} = \frac{\ln(\alpha_2/\alpha_1)}{(\alpha_2 - \alpha_1)} \quad (2.16)$$

Substituting (2.16) into (2.13), one may find

$$\eta = \frac{\frac{\alpha_2}{\alpha_1} - \frac{\alpha_2}{\alpha_1} - \alpha_1 - \frac{\alpha_2}{\alpha_1} - \frac{\alpha_2}{\alpha_2} - \alpha_1}{k(\alpha_2 - \alpha_1)} \quad (2.17)$$

The product  $R_d * C_b$  is found by (3.14) by forming:

$$A1. \alpha_2 = b \text{ and } \alpha_1 + \alpha_2 = a \quad (2.18)$$

Moreover, by the substitution of a and b from (2.8) then we obtain

$$K = R_d C_b = \left( \frac{\alpha_1 + \alpha_2}{\alpha_1 \alpha_2} \right) \left[ 1 - \sqrt{1 - 4 \frac{\alpha_1 \alpha_2}{\alpha_1 + \alpha_2} \left( 1 + \frac{C_b}{C_s} \right)} \right] \quad (2.19)$$

In practice for impulse generators  $C_s \gg C_b$  is always taken in account and for all normalized wave shapes  $\alpha_2 \gg \alpha_1$ . In this conditions (2.19) can be simplified as below:

$$K \approx \frac{1 + \left(\frac{C_b}{C_s}\right)}{\alpha_1 + \alpha_2} \quad (2.20)$$

The substitution of (2.20) in (2.19) finally results in

$$\eta = \frac{C_s}{C_s + C_b} = \frac{1}{1 + \left(\frac{C_b}{C_s}\right)} \quad (2.21)$$

From some calculations, using (2.19) and substituting with required equations the value of efficiency factor for circuit (a) can be obtained as below:

$$\eta \approx \frac{C_s}{C_s + C_b} \frac{R_e}{R_e + R_d} = \frac{1}{1 + \left(\frac{C_b}{C_s}\right)} \frac{1}{1 + \left(\frac{R_d}{R_e}\right)} \quad (2.22)$$

As seen from equation above, by comparison with (2.21) shows the decrease in  $\eta$  due to an additional factor. For this reason, circuit connection (a) is less preferred in establishing of impulse generators.

The dependency of the voltage efficiency factors  $\eta$  with  $C_b / C_s$  ratio is displayed in Figure 2.9 for the standard lightning impulse voltage 1.2/50  $\mu\text{sec}$  as well as for some other wave shapes.

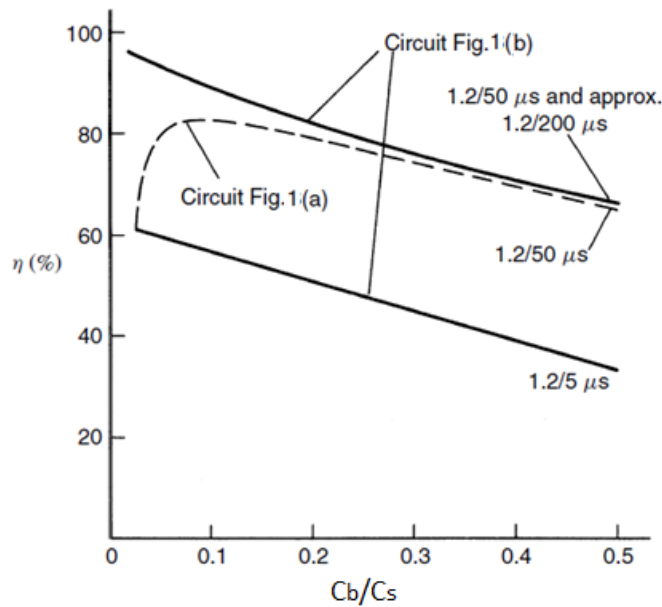


**Figure 2.9:** Voltage efficiency factor  $\eta$  in dependency of capacitance ratio  $C_b / C_s$  for lightning impulse  $T_1/T_2$ .

Since in general  $C_2$  and  $C_1$  are known because of desired power of impulse voltage generator that is under establishing, the common task is to find the resistor values for  $R_1$  and  $R_2$ . For larger generators, the discharge capacitors are always given and dimensioned for a good efficiency (see (2.21) and (2.22)) within a certain range of  $C_2$ .

## 2.5 Multi-Stage Impulse Generators

Single-stage circuits are not suitable for the generation of impulse voltages greater than a few 100 kV, due to limitations in the physical size of the circuit components in

addition, the difficulties encountered with corona discharges at megavolt dc charging voltages. These difficulties can be overcome by the use of multistage impulse generators, as suggested by Marx in the early 1920s [23]. The functional principle is to slowly charge, a group of capacitors in parallel through high-ohmic resistors and then to rapidly discharge, those in series through spark gaps. Marx originally developed this generator principle for testing of insulators and other electrical apparatuses.

Figure 2.10 shows the circuit design for a multistage impulse generator (here it is a three stage impulse generator), often referred to as a Marx generator after its inventor.

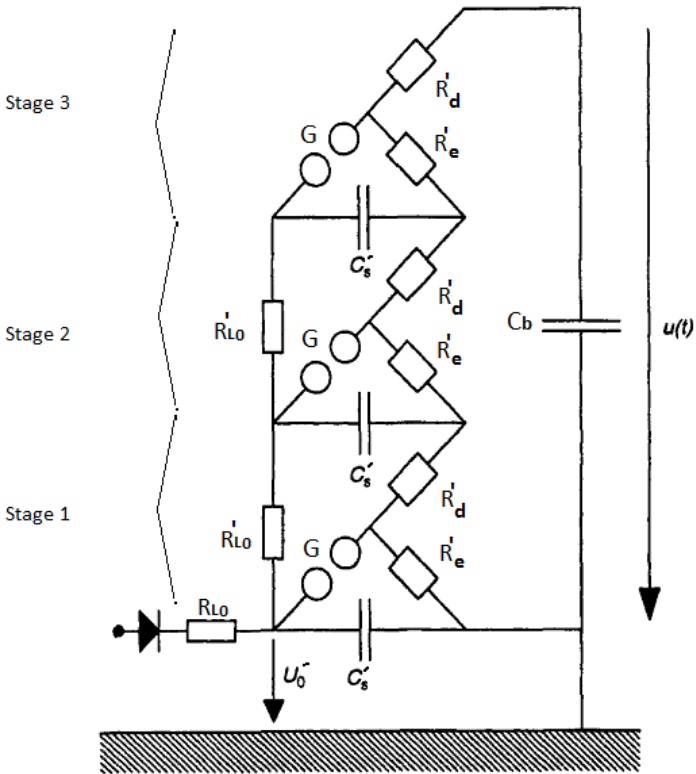


**Figure 2.10:** Multi-stage impulse generator [10].

In fact, each stage of the multi-stage generator is same and is the combination of same single stage generators like what introduced before. As seen in the figure, the example multi-stage impulse generator is composed of single stages in (b) connection. The impulse capacitors of stages  $C'_s$  are charged by a DC charging source to the stage charging voltage  $U'_0$ , via the high charging resistors  $R'_L$  in parallel ( $R'_L \gg R'_e$ ). After a while (depending on stage number and generator

elements values) all impulse capacitors  $C'_s$ , in all stages will be charged through  $R'_L$  to the peak value of  $U'_p$ . Depending on distance between spheres gaps of  $G$  at a proper voltage these switching gaps will breakdown and the capacitors  $C'_s$  will be connected in series. So the load capacitor  $C_b$  will be charging with the series connection of all  $C'_s$ ,  $R'_d$  and  $R'_e$ .

In an  $n$ -stage impulse generator, an equivalent single stage generator can be considered like circuit connection of (b) with the following relationships:

$$U_0 = n U'_0 \quad (2.23)$$

$$R_d = n R'_d \quad (2.24)$$

$$R_e = n R'_e \quad (2.25)$$

$$C'_s = \frac{1}{n} C'_s \quad (2.26)$$

The operation of a multi-stage impulse generator requires that all the spark gaps ( $G$ ) operate almost simultaneously. Therefore, the distances of the spark gaps are set to a value slightly above the natural breakdown at the charging voltage  $U'_0$ . The spark gap of the lowest stage is then triggered either by moving the spheres together or by applying an impulse to a trigger electrode inserted into the first-stage sphere gap.

Firing the impulse generator can be accomplished in three ways:

By slowly charging the stages until the gaps break down and the generator produces an impulse. Slow charging of the generator starts again, the mechanism repeats itself and the generator produces an impulse every minute or so. The reproducibility of the impulse voltages, however, is unsatisfactory.

The first sphere gap is triggered by passing a metal rod between the spheres. This yields a good reproducibility, but the instant of firing is still not well defined.

In order to determine the exact moment of firing, so that the time sweep of oscilloscopes and other measuring equipment can be tripped, a triggered sphere gap according to figure 2.10 is used. A trigger impulse in the order of 10 kV is used to break down the annular gap. This causes a distortion of the main field, ultra-violet

radiation fills the gap and a source of charged particles occurs at the triggered electrode, so that breakdown of the main gap is initiated.

In all these cases, the gaps should be in line and the gaps should “see” each other. Thus, the ultra-violet light of the first gap irradiates the others so that breakdown is initiated. If the radiation is blocked, the firing of the generator will be inconsistent and often be incomplete. Internal oscillations are prevented by dividing the front resistors  $R_f$  over the stages. It would have been more practical to concentrate the front resistance  $\sum R$  in series with the generator; however, stray inductance would cause oscillation within the stages, which would spoil the wave-shape and even cause break down of the discharge capacitors. The triggering system will be discussed in details in chapters 4 and 5.

The equipment for fencing, earthing and shielding research laboratories for high voltages is intended to prevent risk to persons, installations and apparatus. At the same time, undisturbed measurement for rapidly varying phenomena should be ensured and desirable mutual interference between the experimental setup and the environment avoided.

## **2.6 Fencing The Test Area**

The actual danger zone of the high voltage circuit must be protected from unintentional entry by walls or metallic fences. Simple barrier-chains or the identification of the danger zone solely by warning signs can be considered sufficient only where their observation can be constantly switched-off.

Visible metallic connection with earth must be established before the high-voltage elements are touched. In the case of smaller experimental setups, such as a practical, this can be done before entering the setup with the help of insulated rods introduced through the fencing mesh, and with establish the ground connection inside. In larger setups placing the earthing rod should be the first action after entering the danger zone, or automatic earthing switches should be provided. Complete earthing is especially important when the circuit contains capacitors charged by direct voltage [7].

## 2.7 Earth Equipment

Apart from the obvious measures to guarantee reliable earth connections for steady working conditions, one must remember that rapid voltage and current variations can occur during high-voltage experiments because of breakdown processes. In consequence, transient currents appear in the earth connections and this can cause potential differences of the same order of magnitude as the applied test voltages.

Elements at earth potential during steady operation can temporarily acquire a high potential, though in general personal risk is not the consequence. On the other hand, damage to equipment and disturbance of measurements often takes place.

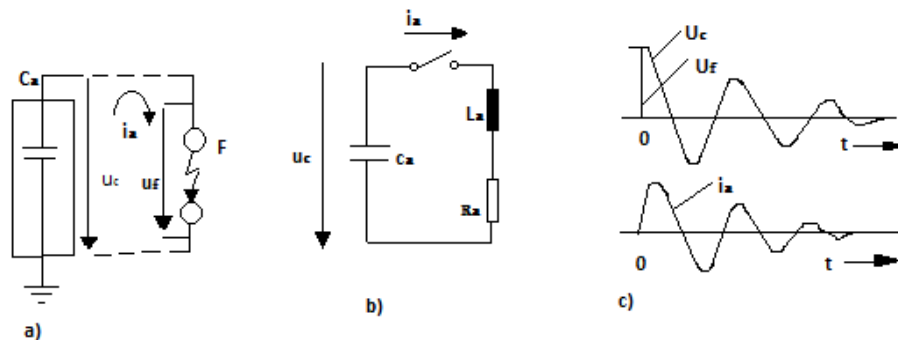


**Figure 2.11:** Earthing in high voltage laboratory [7]

The sudden voltage collapse on breakdown discharge occurs in such short times, that even lightning impulse voltage appear to be slow by comparison. The discharge, which develops at the breakdown discharge site is, to a first approximation, fed by discharge of a capacitor, which, in the case of an impulse voltage generator is essentially the load capacitance and for a testing transformer the capacitances of the high-voltage winding and the test setup. Significant properties of this of affairs can be inferred from the simple scheme of figure 2.11-a capacitor  $C_a$  begins to discharge at  $t = 0$  through a gap which can be bridged in a very short time. The electrical behavior of the circuit can be described by means of the equivalent circuit shown, where  $L_a$  denotes the inductance of the entire chopping circuit. The indicated periodically damped form of the capacitor voltage  $U_c$  and current “ $i_a$ ” results. The first immediately recognizable requirement is that the path of the current “ $i_a$ ” should be closed in an appropriate circuit

An electric field develops between the elements at high-voltage potential and the neighboring elements at earth potential. This stray earth field can be simulated by a distributed earth capacitance  $C_e$ . Should  $C_e$  be rapidly discharged, a transient earth current  $i_e$  is produced, generated by the potential variation of the chopping circuit; this current flows at least in part outside the test setup and here may cause undesirable overvoltages. If on the other hand the entire high-voltage circuit is surrounded by a closed metallic shield, a Faraday cage as in figure 3.6b, then the earth currents too flow in predetermined paths and the earth connections outside the cage remain current-free. These earth connections can therefore be designed exclusively according to the requirements of adequate steady operation grounding.

As a rule the floor of the laboratory is covered at least within the region of the high-voltage apparatus, by a plan earth conductor with as high a conductivity as possible (foil or closely meshed copper grid). The earth terminals of the apparatus are connected to it non-inductively using wide copper bands, to keep the voltage drops due to large currents at a minimum. All measuring and control cables, as well as earth connections, should be laid avoiding large loops and if possible even run underneath the plane earth conductor, e.g. in a metallic cable duct.

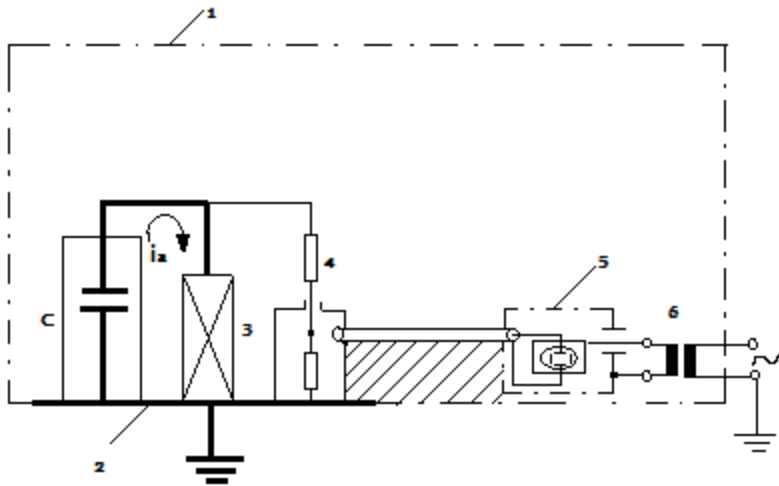


**Fig 2.12:** Earthing and shielding of a high-voltage research setup

In the figure 2.12:

- 1. Faraday cage
- 2. Reinforced plane earth conductor on the floor



3. Test object
4. Voltage divider
5. oscilloscope enclosure or measuring cabin
6. Power supply to osc via isolating transformer and low-pass filter when necessary.

Particular attention should be paid to the connection of the oscilloscope if disturbances during the measurement of rapidly varying phenomena are to be avoided. The measuring signal is always transferred to the measuring device via shielded cables-coaxial measuring cables as a rule. Here by one should however prevent currents, which do not return in the inner conductor, from flowing in the earthed sheath of the measuring cable, since the corresponding voltage drop is superimposed on the measuring signal as an interference voltage.

Interfering sheath currents can be prevented in various ways. If possible the highly conductive plane earth conductor on the laboratory is made large enough so that the cable sheath, adjacent to it and connected with it electrically at several points, is relieved of disturbing current. Better still is the installation of the measuring cable outside the Faraday cage, e.g. in a metallic cable duct or in an earthed metal tube.

It is however often unavoidable that the measuring cables sheath and the earthing system form a closed loop in which disturbing circulating currents may flow because of rapidly varying magnetic fields. An earth loop of this kind is indicated by the hatching in figure 2-3 for the example of a voltage measurement. The oscilloscope enclosure in this case may only be connected by the measuring cable to the earth end of the divider and earthed. that too is why the line input of the oscilloscope has to be fed in via an isolating transformer. This isolating transformer is expedient in any case since potential differences are always present between the earth lead of the mains and the earthed parts of the experimental setup. The disturbing sheath currents may be reduced further by placing ferrite cores over the measuring cables.

In high-voltage setups with very rapid voltage variations electromagnetic waves occur, the interference signal of which may directly affect the measuring cable and the oscilloscope.

For these reason the cable and the oscilloscope used should be really well shielded. Particularly in the case of an oscilloscope with an amplifier, it is advisable to set it up

in a shielded measuring cabin whose line input is fed through an isolating transformer and a low-pass filter.

These same aspects which apply for the connection of oscilloscopes should be observed when direct read-out electronic peak voltage measuring devices are employed. The measurement of impulse voltages chopped on the front is particularly critical.

The peak values of the earth current  $\hat{I}_e$  to be expected under unfavorable conditions rise nearly in proportion to the instantaneous value  $u_d$  of the chopped voltage. The following guiding values have been obtained by experiment:

For incompletely shielded setups  $\hat{I}_e/u_d \leq 2.5 \text{ kA/MV}$

For completely shielded setups  $\hat{I}_e/u_d \leq 6.5 \text{ kA/MV}$

The peak values of  $i_a$  can be very different and usually lie well above  $\hat{I}_e$ . The chopping and the earthing circuit can approximately be interpreted as coupled series resonant circuits; their natural frequencies lie in the region of about 0.5 - 4 MHz. For a given earth current, the impedance of the plane earth conductor is the decisive factor for a voltage drops produced.

## **2.8 Shielding**

Extremely sensitive measurements are often performed in high-voltage experiments. Partial discharge measurements in particular can be disturbed when the extended arrangement of high-voltage circuit behaves as an antenna and receives external electromagnetic waves. Moreover, electromagnetic waves are also produced during breakdown discharge processes in high-voltage circuits, and these can in turn affect disturbance of the surroundings. Practice has shown that the disturbing influence of the surroundings on sensitive high-voltage measurements is generally more intense than that exerted in turn by the high-voltage investigations on the surroundings. This is mainly because disturbing pulses occur in high-voltage circuits only occasionally and are short-lived, whereas the external disturbances, for example due to improperly screened vehicles or electric motors, generate permanent interference.

Almost complete elimination of external interference and at the same time of eventual environmental influences is achieved by using unbroken metallic shielding

in the form of a Faraday cage. The standard required of the plane conductor used for this is appreciably different from that set for the plane conductor in the floor of high-voltage laboratories. Whereas for conductors intended as back-circuit for the transient current the requirement of a low voltage drop is the primary consideration, high damping of the electromagnetic fields is the objective in plane conductors intended for shielding purposes. It will therefore usually be sufficient if a close-meshed metal net is hung on or set into the walls of the laboratory and the unavoidable apertures for power and communication leads are blocked for high-frequency currents with low-pass filters. When putting this into practice special attention must be paid to careful shielding of doors and windows [7].

The erection of a complete Faraday cage is certainly desirable in every case, but is absolutely necessary only when sensitive partial discharge measurements are intended. Experiments in a high-voltage practical course can usually be performed without exception in partially shielded setups, which have only one plane earthed conductor in or on the floor of the laboratory.



### **3. MEASUREMENT OF IMPULSE VOLTAGES**

#### **3.1 General Aspect of Measurement**

Measurement is a process of gathering information from the physical world and comparing this information with agreed standards. Measurement is essential in order to be able to observe and test scientific and technological investigations. Instruments are developed for measuring the conditions of physical variables and for converting them into symbolic output forms so that we can interpret and understand the nature of these physical variables.

Recent advances in high voltage engineering increases demands for more especial and accurate tests. High voltage laboratories that perform different sort of tests are asked with producers and national and international standards to bring out more accurate test results. From this aspect, nowadays laboratories equip their test tools with modern and calibrated devices and measuring systems. The subject of this thesis, which is related with impulse tests, includes investigating of measuring systems used in laboratories.

As a rule, voltage dividers are used for the measurement of high lightning, switching and ac voltages. Such voltage dividers have to reduce to some 100 V, i.e. to the normally used measurement or recording value of voltage, high and extra high voltages up to several million volts. While giving on the low voltage side a true reproduction of the high voltage applied to the test object. It would be, in principle, possible to design an optimal voltage divider for any particular voltage stress measurement [9].

In practice, however, HV laboratories must have at their disposal a voltage divider designed for easy handling and being of universal use. Voltages used for acceptance tests of electric equipment in h. v. laboratories are essentially the 1.2/50 lightning impulse voltage, the 1.2/50 front or tail chopped lightning impulse voltage, the switching impulse voltage as well as ac voltage.

The voltage divider and the object under test are generally connected by means of a metal conductor a few meters long, this in view of avoiding any mutual influence. This conductor influences however the transfer ratio quality of the whole measure circuit, so that the transfer ratio of the voltage divider has necessarily to take into account the lead-in connection [14].

Nowadays international recommendations on impulse measurement (IEC 60, I to 4) are completed. Special care was given to the accuracy of the impulse measurement. The measurement of the transfer characteristics was specially dealt with. For practical measurement in any high voltage laboratory the transfer characteristic of the whole measuring system and the different influencing parameters on it are of interest.

High voltage impulse tests are normally performed by the comparison method. Two or more impulse voltage and current records are compared with each other at different voltages. If they show no differences in the wave-shape then the insulation has passed the test. For such measurements, a highly accurate and disturbance-free measuring system is necessary. As an example in impulse test of a high voltage insulator depending on highest voltage that insulator can withstand for, in different voltage levels several test are demonstrated. In each voltage level several tests are done.

### **3.2 Measurement of Impulse Voltages**

The measurement of high voltages in laboratories or power systems is performed with capacitive, inductive or resistive dividers or with a combination of components of these. In hv impulse measurement we can distinguish nowadays between

- Resistive dividers
- Capacitive dividers
- Damped capacitive dividers

In the UHV-range, the damped capacitive divider, consisting of a series connection of resistors and capacitors, is the mainly used design. For the dimensioning of the measuring system in the UHV-range, at first the total impulse circuit needs to be calculated. Therefore the high voltage part of an impulse measuring system has to be optimized taking into account the requirements with respect to the generation of the

desired impulse shapes of the HV circuit and the necessary transfer characteristics in order to measure these impulse voltages. Special consideration has to be given to the economics.

The ohmic voltage divider is limited to lightning impulse voltages up to about 2 MV. For the generation of switching impulse voltages the resistance value is too low if the resistor is dimensioned for the measurement of lightning impulse voltages. The capacitive voltage divider is suitable for switching impulse voltages, but for the measurement of lightning impulse voltages this type of divider cannot be used, because of its tendency to oscillate.

The only type of divider, which can fulfill the IEC-requirements in the UHV range, is the damped capacitive voltage divider. This divider can be dimensioned in two different types:

- Capacitive divider with external damping resistor. This is a solution for the lower voltage range up to 1 MV.
- Series connection of resistors and capacitors in the high voltage arm [13].

The duty of the voltage divider is to reduce the high voltage of some million volts to a voltage of some 100 volts. This low voltage should be an image of the high voltage only reduced by a constant factor, the ratio. The ratio should therefore be independent of e.g. the amplitude of the applied voltage, the temperature, the frequency, the surrounding etc. Then this low voltage can be indicated by an instrument. Recent developments in fiber optic transmission systems have resulted in a measuring system with a spherical electric field sensor, applied now to high voltage impulse measurement.

Figure 3.1 illustrates the common and most adequate layout of any voltage testing circuit.

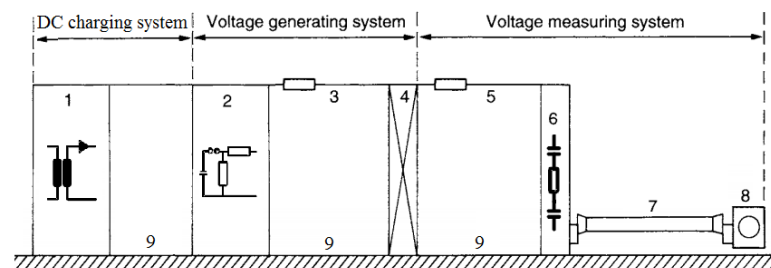


**Figure 3.1:** Basic voltage testing system.

In the figure 3.1:

DC charging unit (1), Impulse voltage generating unit (2), Lead to test object (3), Test object (4), Lead to voltage divider (5), Voltage divider (6), Signal or measuring cable (7), Output recording instrument (8), Ground return (9).

The voltage generator 2 is connected to a test object 4 by a lead 3 that these three elements form a voltage generating system. The lead 3 to the test object may comprise any impedance or resistance to damp oscillations, if necessary, or to limit the short-circuit currents if the test object fails. The measuring system starts at the terminals of the test object and comprises a connecting lead 5 to the voltage divider 6, and a recording instrument 8, whose signal or measuring cable 7 is placed between its input terminals and the bottom or l.v. part of the divider. The appropriate ground return 9 should assure no significant voltage drops for even highly transient phenomena and keep the ground potential to earth as close as possible.

### **3.3 Considerations In Impulse Voltage Measurements**

Following criteria must be considered for the selection of capacitive voltage dividers to be used in test laboratories:

- a) High voltage appearing on the test circuit must be transferred with maximum accuracy to the secondary output of the voltage divider. Coaxial cable on the lv side as well as the measuring instrument (i.e. oscillograph) can be chosen so that they will not further distort the impulse wave shape.
- b) Influence of the voltage divider on the shape of voltage applied to the test object must either be negligible when the voltage divider is used solely as a measuring device or, on the contrary, have an optimum effect, for instance when the divider is simultaneously used as a load capacitor of the impulse test circuit. The latter solution has the advantage of being economic and ensures at the same time a better use of the available space.
- c) The capacitive voltage divider should be easily adaptable to any actual voltage value produced by the impulse generator, connected in parallel or in series, or when only part of the generator stages are used. The accuracy of the transfer ratio should be maintained also in this particular case and it would be an advantage to be able to use the same lv units even if the number of active generator stages is reduced.



d) It should be possible to determine easily the transformation ratio.

Measurement and interpretation of response time should be possible with more or less certitude in view of correcting, by means of this response time, impulse waves chopped in their front. This means that a strongly oscillating or insufficiently attenuated response time curve is not desirable.

The influence of the impedance of a voltage divider on the generation circuit cannot be neglected. Therefore, this impedance has to be dimensioned not only according to the measuring requirements for high impulse voltages but also to the load requirements of the circuit [11].

### 3.4 Transfer Characteristics

In measuring and recording impulse voltages by means of voltage dividers and digital oscilloscope, errors as high as 10% or even higher are usually observed. The errors are not only in magnitude but also in phase. Whatever the equivalent circuit of voltage dividers is, a four-terminal network can represent them, and their transfer characteristics (output voltage/input voltage,  $v_0/v_i$ ) can be evaluated. Practical impulse voltage shapes are the difference between two exponential voltages. The mathematical analysis for such waves is very lengthy and tedious. Checking the response of voltage dividers by applying a unit step function is recommended by IEC. If a unit step function in the form

$$v_i(t) = \begin{cases} 0 & t < 0 \\ 1 & t > 0 \end{cases} \quad (3.1)$$

is applied to a voltage divider, the output response will be  $v_0(t)$ . The response to another input voltage can be derived by Laplace transform, and hence the output in the time domain is obtained. Good design of voltage dividers should provide:

- Short delay time  $T_d$ .
- Low overshoot
- Short time to steady state

In recording impulse voltage waves, the output of the divider is taken via coaxial cables to a digital oscilloscope. Unless proper matching is provided, errors resulting from voltage reflections are introduced.

The main parameters influencing the transfer characteristics (output voltage/input voltage,  $v_o/v_i$ ) of low damped capacitive voltage dividers are:

- The measuring circuit (horizontal lead, square loop arrangement),
- External damping resistor at the beginning of the lead (three-component system, two-component system),
- Impedance of the lead,
- High voltage arm electrodes and active elements
- Low voltage arm
  - .Nominal voltage of low voltage arm
  - .Construction (inductance, coaxial arrangement)
  - .Elements
  - .Earthing connections [10]

According to the standards high voltage apparatus and systems are tested with full and chopped lightning impulses of several hundred kV to a few MV with frequency components up to the MHz range. The HV impulses are usually measured using a divider, which should provide the measuring instrument e.g. an impulse voltmeter, an oscilloscope or a digital recorder, with an exact replica of the HV signal. Due to the limited transfer characteristic of the impulse divider systems, however, including the HV lead to the divider, the output signal on the low-voltage side of the divider may be distorted. This could lead to errors when evaluating the peak value, the front time and other significant parameters of the HV impulse from the divider output voltage.

The transfer characteristic of an impulse divider system is given by its response to a step voltage. The step response being known, the transfer errors of the divider can be calculated for any HV impulse, or, vice versa, the HV impulse can be reconstructed from the distorted signal at the divider output terminals using a numerical deconvolution algorithm. Thus, the voltage and time errors due to the limited transfer characteristic of the divider can be corrected. However, for routine tests with

standardized impulse voltages, there is a great need in practice to characterize the divider using only a limited number of response parameters instead of the complete record of the step response. When the response parameters of the impulse divider are known, the test engineer should then be able to decide whether the divider is suited for the measurement of the test voltage within the specified error limits.

The transfer characteristic of an impulse divider system is given by its response to a step voltage. The step response being known, the transfer errors of the divider can be calculated for any HV impulse, or, vice versa, the HV impulse can be reconstructed from the distorted signal at the divider output terminals using a numerical deconvolution algorithm. Thus, the voltage and time errors due to the limited transfer characteristic of the divider can be corrected. However, for routine tests with standardized impulse voltages, there is a great need in practice to characterize the divider using only a limited number of response parameters instead of the complete record of the step response. When the response parameters of the impulse divider are known, the test engineer should then be able to decide whether the divider is suited for the measurement of the test voltage within the specified error limits.

Several response parameters are known in the various literature and some of them are accepted in the present standard for impulse voltage tests. However, as there are different types of impulse dividers, e.g., resistive, capacitive and damped capacitive ones having stray capacitances and residual inductances, their step responses show quite different temporal shapes. This makes it difficult to define a universal response parameter or appropriate set of parameters, which can substitute the step response in characterizing the transfer errors of a divider. After long experience with these response parameters, the adequacy of the specification has been discussed and other response parameters have been proposed for introduction in to the revised standard.

Now the parameters needed for the dividers, are experimental response time  $T_n$ , the partial response time  $T_a$ , the initial distortion time  $T_0$ , the over shoot  $\beta$  and the settling time  $t_s$  [9].

### **3.5 Unit Step Response**

To evaluate the parameters needed for the dividers, the most used response is unit step response, which in general is defined as:

$$g(t) = \begin{cases} 0 & \text{for } t < 0 \\ 1 & \text{for } t > 0 \end{cases} \quad (3.2)$$

To apply this function for a voltage divider the simplest setup configuration can be showed as in figure 3.2. In a square loop arrangement, the divider is connected to the step generator via a horizontal and a vertical lead, each as long as the height of the divider.

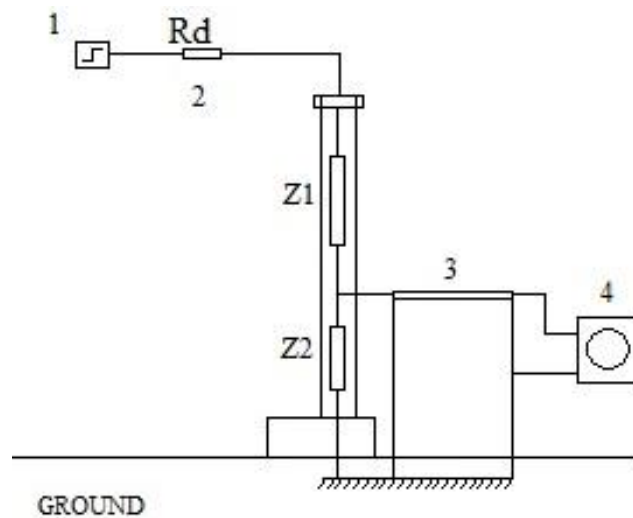


**Figure 3.2:** Unit step response setup.

In figure 3.2, 1 is unit step generator, 2 damping resistor, 3 connecting cable (coaxial cable), 4 digital oscilloscope,  $Z_1$  HV impedance and  $Z_2$  is lv impedance.

The idealized unit step response  $g(t)$  of an oscillating system is showed in figure 3.3 But the "experimental step response" so obtained is, in general, not equal to the step response of the divider in the actual HV test circuit, which is quite different from the step response measurement arrangement [13]. In the theoretical considerations, point o in the curve of figure 3.3 is chosen as that instant when the response first deviates from zero and it is called "the true foot point". In practice, this point would need a precise method of determination, which is difficult to achieve due to the presence of disturbances. The instant  $t_1$ , is when the unit step response first passes unit amplitude. The following parameters crystallized as those which best represent response errors.

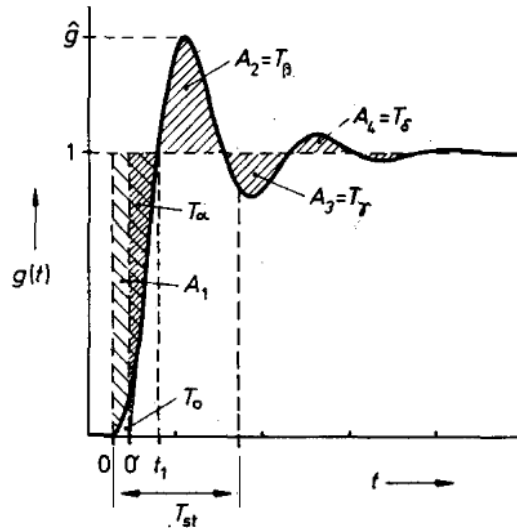


**Figure 3.3:** Idealized unit step response of an oscillating system with virtual origin.

Since the dividers in laboratories are generally unshielded, it is susceptible to electromagnetic interference. This may lead to bumps or oscillations superimposed on  $g(t)$  at the beginning. In order to eliminate this interference, the IEC standard defines a virtual starting point  $0'$ , by the intersection of the time axis and a straight line drawn as a tangent to the steepest portion of the front of the experimental step response (as it can be seen in Figure 3.3). This definition is somewhat arbitrary, and significant information about  $g(t)$  may be lost by replacing its original shape by a straight line [13].

As mentioned before, ignoring for virtual origin proposed by IEC the unit step response of figure 3.3 can be showed as figure 3.4.

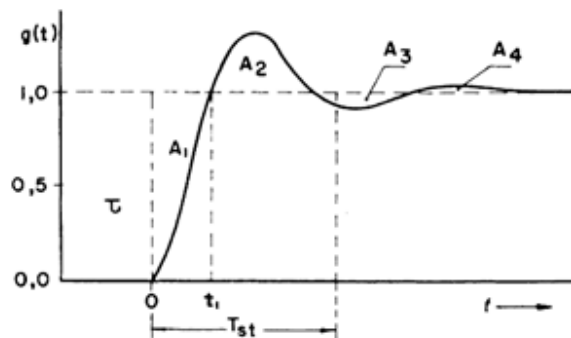


**Figure 3.4:** Idealized unit step response of an oscillating system without virtual origin.

Regarding to curve of figure 3.4 the response parameters of unit step response can be written as:

$$T = \int_0^{\infty} (1 - g(t)) dt = A_1 - A_2 + A_3 - \dots \quad (3.3)$$

Where T is the response time, which is difference of lower areas from uppers.

$$T_n = T_\alpha - T_\beta + T_\gamma - \dots \quad (3.4)$$

Where  $T_n$  is experimental response time,  $T_\alpha$  is partial response time which is given by the first partial area of the step response starting with the tangent from the virtual starting point 0' (Figure 3.3). The value of  $T_\alpha$ , gives information about the immediate response of the divider to fast voltage changes and to high frequency oscillations superposed on the hv impulse. The partial response time is restricted to  $T_\alpha \leq \frac{2}{\pi f_{max}}$  where  $f_{max}$  is the maximum frequency of oscillations that may reasonably occur in the circuit [14].

$$T_s = \sqrt{2 \int_0^{\infty} t (1 - g(t)) dt} - T^2 \quad (3.5)$$

Where  $T_s$  is standard rise time.

$$T_{re} = - \int_{t_1}^{\infty} (1 - g(t)) dt = A_1 - T \quad (3.6)$$

Where  $T_{re}$  is the residual time.

$$T_{st} = \frac{1}{k} \left| \int_{T_{st}}^{\infty} (1 - g(t)) dt \right| \quad (3.7)$$

Where  $T_{st}$  is time to steady state and constant  $k = 0.02$ .

According to IEC standards, the response time, T, as given by (3.3), represents several important features. First, T represents the sum of the partial areas between  $g(t)$  and the unity level (Figure 3.3). Secondly, for any step response defined by (3.2), T represents the time delay of the divider response to any input voltage when the steady state has been reached, which it means we will have same delay while measuring any impulse voltage generated by impulse voltage generator. Furthermore,

the instantaneous voltage difference between an input ramp and the response in the steady state is given by

$$\Delta U = ST \quad (3.8)$$

Where S is the ramp slope [13].

This simple relation can be used for the calculation of the crest value of front-chopped impulses from the divider response, or for the determination of T instead of (3.3) [14].

The IEC standard takes account of the inadequacies in measuring the step response of an HV impulse divider system. According to (3.3), an experimental response time, T, is defined which is evaluated from the experimental step response measured in the square loop arrangement of figure 3.2. The vertical lead connecting the generator to the divider affects the divider response. From T, the response time of the divider system in the HV circuit including the horizontal HV lead can be obtained by the correction for the effect of the vertical lead

$$T = T_n + \tau v \left(1 - \frac{Z}{R}\right) \quad (3.9)$$

Where  $\tau v$  is the propagation time along the vertical lead, Z is the characteristic impedance of the vertical lead, and R is the resistance between the top of the divider and the ground. The response time defined in (3.9) is not identical with that in (3.3) which is due to the differing starting points 0 and 0' as shown in figure 3.3 and 3.4 [13].

Assuming the virtual origin, The parameter initial distortion time,  $T_o$ , can be defined as the area between  $g(t)$  and the straight line used to determine 0' (Figure 3.3).  $T_o$  should be below in order to limit additional errors in crest voltage measurements of front-chopped impulses.





## **4. TRIGGERING SYSTEM OF IVG**

### **4.1 Trigatron**

There is a frequent need for a high-voltage switching capable of rapid and controlled operation over a considerable voltage range. This need arises, for instance, in the operation of impulse generators, in the production of 'chopped' impulse voltages and in the diversion of the discharge energy when electrical breakdown occurs in equipment under test. In the latter case, the energy dissipated may frequently be destructive, preventing further tests on the particular test object. For instance, in the experiments to determine the electric strength of insulating oil, each breakdown causes a deterioration of the insulating properties and limits the number of measurements possible on a sample. Below about 10 kV, power electronic devices can perform the various switching operations outlined above. Using such devices, the discharge energy of a breakdown, for example, may be diverted from the test object in times of less than one microsecond. Above this voltage, it is usually necessary to resort to a spark gap in air as the switching device, and to provide a third electrode as the control or trigger. One such three electrodes spark gap is the trigatron, consisting of two hemispherical main electrodes, together with a trigger electrode of small diameter mounted centrally in a hole in one of the main electrodes, and insulated from it (see Figure 4.1). A comparatively small voltage applied to the trigger electrode can cause the main gap to break down at voltages below the normal sparking voltage. The device is thus a controlled switch. The development of trigatrons for use as modulators in recurrent-pulse equipment, in which the requirements are those of high repetition rate and freedom from jitter, has been well described by Craggs, Haine and Meek [16].

The trigatron spark gap was invented in the early 1940's by Craggs, Haine, and Meek to serve as a switch in high-power modulators for radar, and has found wide application as a high voltage, high current switch. A trigatron spark gap has three electrodes, two of which form the main gap. The third, the trigger pin, is located inside a hole in one of the main gap electrodes. In operation, a voltage less than the

static main gap breakdown voltage, VSB, is applied to the main gap and breakdown is triggered by the application of a voltage pulse to the trigger pin. There are different agreements about the physical mechanism responsible for triggering breakdown of the main gap. The most common view in the technical literature is that the breakdown of the main gap is initiated after the gap between the trigger pin and the adjacent main gap electrode breaks down, and is the result of the action of this spark. Another viewpoint is that breakdown occurs because of the formation of a streamer in the distorted field around the trigger pin tip before the formation of the trigger spark [20].

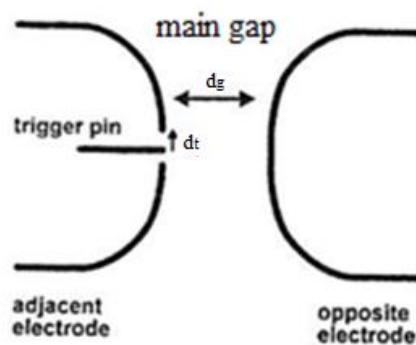


**Figure 4.1:** Typical trigatron system.

In these first papers, the dependence of the operating characteristics on the voltage polarity configuration was reported [16], and the exceptional voltage operating range of the device noted. Both blown and sealed devices capable of operation at repetition rates exceeding 1 kHz were reported. Craggs, Haine, and Meek linked the triggering mechanism to "the concentration of the voltage gradient in the region of the trigger wire on the application of the trigger pulse," but attributed the triggering of breakdown to effects of the trigger spark that forms between the trigger wire and the adjacent main gap electrode upon- application of the trigger pulse [18].

Several later reports of studies of trigatron operation have appeared. Of these studies, most attributed the initiation of breakdown to the action of the discharge between the trigger pin and the adjacent main gap electrode. The most common view was that the action of the trigger spark produced a discharge in the main gap, through a Townsend-like mechanism, followed in some cases by a transition to a streamer or Kanal mechanism. Depending on the polarity of the main gap charging voltage, the Townsend-like discharge was thought to be initiated by electrons produced by

photoemission from the distant cathode, photoionization of the gas in the gap, or drift from the plasma of the trigger spark. These electrons would create others through electron impact ionization, and eventually cause either the formation of a transient glow discharge between the main gap electrodes or a streamer. Further heating would then occur to form the arc and close the switch. Some other authors proposed that another factor in the breakdown of the nominally undervolted main gap resulted from the expansion of hot gases from the trigger spark into the main gap region. Because at a fixed pressure the molecular (or atomic) number density of a gas decreases with temperature,  $E / N$  and therefore the Townsend ionization coefficient  $\alpha$  would be higher in the hot gas. Saxe proposed a similar mechanism, but invoked the shock wave propagating outward from the trigger spark to produce the enhanced  $E / N$  [20]. Craggs et al suggested that triggering might be due to the field distortion around the trigger pin tip. Subsequent authors generally discounted this mechanism; however, on the basis that breakdown of the main gap in many cases occurred after the breakdown of the trigger gap. They reasoned that since the voltage on the trigger pin collapses upon breakdown of the trigger gap, the breakdown process in the main gap must be arrested at the same time if it is initiated by field distortion. In a remarkably insightful paper, Shkuropat noted that the clear dependence of trigatron behavior on the relative polarities of the trigger and main gap charging voltages is difficult to explain with mechanisms of this type. Triggering was almost universally observed to be better with the heteropolar configuration than with the homopolar. Since the voltage on the trigger pin collapses upon breakdown of the trigger gap, this difference is difficult to explain in terms of a model in which all the action occurs after this collapse. Based on experiments conducted with almost 100 kV trigatron, he concluded that, at least for charging voltages resulting in rapid triggering, the initiating events occur before the collapse of the trigger gap voltage, and suggested that a streamer initiated directly from the enhanced field around the trigger pin tip was involved. With this model, it is only necessary that the trigger gap not breakdown until after the streamer has been initiated and, perhaps, traversed some portion of the gap. Further experiments reported in a later paper supported this model, and explored the transition from streamer to arc channel [18].

In this model, the enhanced field near the trigger pin tip launches a streamer that propagates across the gap, bridging it with a low-conductivity channel. This channel

then heats to form the arc, which closes the switch. Propagation of the streamer tip depends on the presence of an enhanced field ahead of it. This field is determined by a number of factors, including the algebraic difference between the potential of the tip and that of the opposite main gap electrode. Since the tip is connected to the trigger pin through the streamer channel, before the trigger potential collapses this difference is substantially larger for a heteropolar than for a homopolar configuration. This fact then explains qualitatively the observed dependence of trigatron characteristics on polarity configuration. Further, the model predicts that increasing trigger voltage will improve triggering only up to that point where the trigger gap breaks down before the streamer has traversed the gap. Thus the design of an optimum triggering system involves balancing the requirements of maximizing the field enhancement near the trigger pin tip, with delaying the breakdown of the trigger gap at least until a streamer can be formed and propagate across the main gap. Shkuropat reported behavior consistent with this prediction.

In a series of papers, Yoshida and Sugita reported the results of experimental and numerical modeling studies of trigatrons. They proposed that two distinct modes of breakdown exist, which they refer as longitudinal trigger and side trigger. The longitudinal trigger mode is similar to that discussed by Shkurcpat and the side trigger mode is similar to the mode proposed in the earlier papers. No explanation was provided as to why the longitudinal mode is observed in some cases and the side mode in others, and they reported that their gap operated only in the side trigger mode. Further, Yoshida and Sugita presented time-resolved shutter photographs of the emission from the gap during triggering. These photos show diffuse regions of luminosity propagating from the trigger to the opposite main gap electrode at a speed of almost 108 cm/s, too fast to be due to electron drift. Although Yoshida and Sugita interpret these data in terms of the side trigger mode of operation, they seem actually to be more supportive of the longitudinal mode instead [18].

El'chaninov et al and Emel'yanov et al have published results of experimental studies of high-voltage (400 kV to 1.9 MV) trigatron operation. Using up to eight trigger pins in the same gap, these authors report simultaneous closure through multiple arc channels with Current closure with current sharing between the arcs. The design of their gaps was based on the streamer-initiated breakdown model, and they presented experimental results supporting the validity of it. Particularly convincing are

measurements of closure delay versus trigger voltage that show that the delay first decreases, then increases with increasing trigger voltage, similar to the results of Shkuropat. In later work, Kremnev, Novakovskii, and Potaliisyn studied arc channel formation in a high-voltage trigatron with nanosecond time resolution, and presented shadowgraphs of the developing arc channel in nitrogen for charging voltages between about 80% and 200% of static self-break.

Wootton studied a trigatron spark gap operating near the minimum triggerable main gap voltage, and concluded streamers initiated that main gap breakdown. He presented photographic evidence showing that the main and trigger gap arcs connected to different points on the surface of the trigger pin, and developed a triggering map that clearly showed the deleterious effect of too high a trigger voltage, causing early breakdown of the trigger gap.

Martin has developed a phenomenological description of breakdown, which he has applied to a number of devices, including trigatrons. The description is based on a model in which breakdown is initiated by a streamer (which he calls a fast discharge) crossing the gap, and completed by a heating phase in which the weakly conducting channel left by the streamer is transformed into an arc. Working with Martin, Wells obtained photographs that show the filamentary nature of the initiatory processes in a trigatron [21].

## **4.2 Mathematical Aspect of Trigatron System**

The trigatron switch has long been used in the switching of large currents. A particular advantage of the geometry, with the trigger pin concentric and within one of the two electrodes, is that a relatively low trigger voltage is required to initiate the discharge. A schematic diagram of the trigatron switch is shown in Figure 4.1. The three electrodes, the opposite electrode, the adjacent electrode and the trigger pin are shown in the figure. Conventionally the opposite electrode is live and the adjacent electrode is at earth potential. The switch is operated by applying a trigger voltage,  $V_t$  to the trigger pin, normally in the earthy electrode, in the presence of the main voltage,  $V_g$ , on the live electrode. The closure of the switch therefore involves two gaps, the trigger gap, of width  $d_t$  between the trigger pin and the adjacent electrode, and the main gap, of width  $d_g$ , between the trigger pin and the opposite electrode. When the volts are applied, the mean electric fields between the trigger pin and the

adjacent electrode ( $E_t$ ) and between the live electrode and the trigger pin or adjacent electrode ( $E_g$ ) are given by (4.1) [21]:

$$E_t = V_t / d_t \quad \text{and} \quad E_g = (V_g - V_t) / d_g \quad (4.1)$$

Discharge in the trigatron can be initiated along two distinct routes as shown in figure 4.2. The voltage on the trigger pin can cause a breakdown to the adjacent electrode (BAE) with the resulting UV and charged particles initiating the discharge across the main electrodes. Or the same voltage can create a distorted and enhanced field in conjunction with the applied voltage across the main gap, resulting in the formation of breakdown streamers directly across to the opposite electrode (BOE) [20]. BOE is a fast-breakdown mode that when the trigger pulse is applied to the trigger pin, the breakdown between the trigger pin and the opposite electrode takes place first. After the main-gap voltage has collapsed, the breakdown of the trigger gap will generate under a high degree of overvoltage. BAE is a slow breakdown mode that the breakdown across the gap between the trigger pin and the adjacent electrode takes place first. The intense UV radiation is believed to produce free electrons through photoionization. Afterward, the initiation of an electron avalanche in turn leads to the breakdown of the main gap. The advantages of BOE are short breakdown time and low jitter, but its defect is serious erosion of trigger pin because of the main current passing through the trigger pin in initial discharge. On the contrary, BAE would have a long lifetime with low erosion, although the breakdown time is relatively long with microsecond level [21].

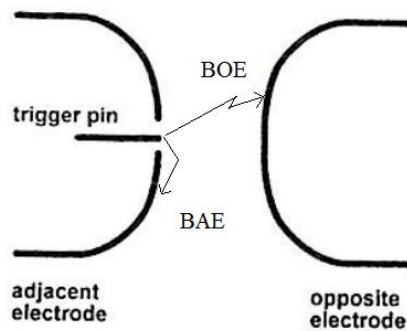


**Figure 4.2:** Two possible way for discharge in trigatron.

Time delay can be defined as the time between the trigger pulse arriving at the trigger pin and the voltage on the main gap starting to decline. The time delay can be

divided into two parts, i.e., the rise time of the trigger voltage  $t_r$  and the breakdown time of the main gap  $t$ . Time delay can be written as:

$$t_d = t_r + t \quad (4.2)$$

As for the fast-breakdown mode (BOE), it can be given that  $t \ll t_r$ . As for the low-breakdown mode (BAE), it can be given that  $t \gg t_r$ . Here the breakdown time means the breakdown time of main gap  $t$ , and it can be measured by monitoring the voltage shape on the trigger pin and the HV electrode.

Depending on discharge model (BOE or BAE) from a large range of data including that from electrically triggered, laser triggered, and untriggered gaps some relationship can be derived. On applying this relationship to the trigatron configuration the condition for BOE or BAE operation of the switch is evident. If the trigger and main voltages on the switch are such that  $|E_t| > |E_g|$  then the trigger pin will break first to the adjacent electrode (BAE) and conversely if  $|E_t| < |E_g|$  the trigger pin will break first to the opposite electrode (BOE). The magnitude of the mean electric field across the two gaps is equal when the trigger voltage is equal to  $V_t^*$ , given by (4.3):

$$V_t^* / V_g = d_t / (d_g + d_t) \text{ for the same polarity } V_t \text{ \& } V_g \quad (4.3a)$$

$$V_t^* / V_g = -d_t / (d_g - d_t) \text{ for opposite polarity } V_t \text{ \& } V_g \quad (4.3b)$$

Consequently for trigger voltages with magnitudes greater than  $|V_t^*|$ , BAE operation will occur, while for trigger voltage magnitudes less than  $|V_t^*|$ , BOE operation will take place [15].

In the past several years, there are amounts of reports about the related research, including the influence factors on characteristics of the switch. Among these characteristics, the breakdown time attracts much attention since it is an important performance for the switch. In general, E-field enhances near the trigger pin because of extremely nonuniform E-field distribution. For the conventionally used position of the trigger pin low or ground, the E-field is generally 2–2.5 times the mean E-field of the main gap [15].

When the volts are applied, initiated electrons emit from the cathode. These electrons are accelerated and move to the anode or trigger pin caused by the E-field, which in turn leads to electron collisions and avalanches. In general,  $V_g$  is much larger than the breakdown voltage between the trigger electrode and earthen main electrode. Therefore, streamer is harder to form at anode than that of the trigger pin because of its smaller E-field, which was confirmed by high sensitivity-streak camera photograph.

Furthermore, the second emission effect can also be neglected since the breakdown time is so short (nanosecond or microsecond). Therefore, the contribution to the breakdown for electrons moving toward to anode is believed to be less. On the other hand, because of the effect of E-field enhancement, the electrons moving to the trigger pin form streamer more easily, inducing the collapse of the switch [21].

The discharge of the trigatron and its mechanism will be discussed in details in the preceding paragraphs but here to help our formulation we accept that the initial discharge of the trigatron can be considered as corona discharge. Therefore, the breakdown of the nonuniform E-field is generally developed from corona discharge to spark discharge. Therefore, the trigatron can be simplified as a negative plate electrode–positive stick electrode mode, i.e, supposing the shape of the cathode is plate, neglecting the aberrance of the E-field caused by earth electrode since the role of this aberrance of the E-field is not important and the aberrance of the E-field caused by electrode shape.

The main products of this trigger spark are as follows:

(a) A local region of hot gas of low density, corresponding to the spark channel, which would be ejected into the main gap and would continue to move after the trigger discharge had ceased. The initial growth of the spark channel can be about  $10^{-5}$  cm/sec or greater, and is accompanied by a shock wave. Behind this, the low-density region would tend to propagate at lower velocities.

(b) Ionization products, electrons and positive ions. The electrons may not be as important as the relatively immobile positive ions, which can produce important space charges. These charged particles may be ejected along with the hot-gas region.



(c) Photons that will irradiate the main gap. These will be very important in ensuring an initial supply of electrons, particularly at the opposing main electrode. The efficacy of spark illumination in photoelectron production is well known.

(d) Hot electrode spots, especially at the trigger cathode, which will continue to emit electrons for an appreciable time after the trigger discharge has ceased [21].

A combination of these processes might be expected to produce significant values of  $\alpha$  (electron ionization rate coefficient) at least in the low-density region of expelled gas, and it is then possible to give a reasonable explanation for the majority of the effects found. The essential feature that permits breakdown below  $V_s$  (static breakdown voltage of the trigatron gap) appears to be the injection of the hot low-density region into the gap. Such a region is likely to persist for long periods (about  $10^4$  sec), as is found from studies of dielectric recovery following arc extinction in circuit interruption [21]. It provides a region in which ionization by electrons can occur readily and one in which positive-ion space charge builds up. It is suggested that the production of a space charge in this way, which moves out as the low-density region moves, causes the onset of a main-gap breakdown, which itself proceeds by a more normal breakdown process. The simultaneous supply of photoelectrons aids this process considerably in fact, at potentials just below  $V_s$  the photoelectrons alone would cause breakdown. Triggering of spark gaps by photons has been reported at potentials of 0.9 V but below this, and especially near  $u_0$  (lower limit of operation or triggering limit), these alone would not be effective. Deferring for the present a more detailed consideration of the trigger region, two modes of operation in the main gap may be distinguished, according to polarity [16].

During these processes if the E-field is high enough, the breakdown between the negative live electrode and the trigger pin can be divided into three stages.

(1) The electrons emit from the cathode and result in avalanche. The electrons moving distance  $x$  from avalanche to streamer can be calculated from Raether breakdown criterion

$$\alpha x = 17.7 + \ln x \quad (4.4)$$

Where  $\alpha$  is the electron ionization rate coefficient, which is dependent on the electric E and pressure of the filled gas p,

$$\frac{\alpha}{p} = A_e - B_p / E \quad (4.5)$$

The minimum broken voltage for free electrons developed to an electron avalanche can be calculated from (4.6)

$$U_b = \frac{Bpdg}{\ln\left[\frac{Apdg}{\ln\left(1 + \frac{1}{\gamma}\right)}\right]} \quad (4.6)$$

Where A, B, and  $\gamma$  are constants, which are related to the cathode material. If the cathode material and gas are decided, A, B, and  $\gamma$  can be determined by approximating the experimental curves [21].

(2) If the broken E-field is near the self-breakdown value, after electrons are absorbed by anode, it results in positive ions leaving in the front of the anode. A positive streamer forms, which is from anode to cathode. Supposing the radius of the electron avalanche head is  $r'$ , the criterion for this streamer spontaneously spread is

$$\int_r^R \frac{2}{3} \eta f \mu e^{-\mu\rho} \frac{r\sqrt{\rho}}{(d_g - x_1)^{1/2}} \alpha(x, \rho) e^{\int_r^{\rho} \alpha(x, \rho') d\rho'} d\rho = 1, \quad (4.7)$$

Where R is radius of the sphere, in which electrons participate in the formation of streamer.  $\eta$  is the coefficient of photoionization, f is ratio of the excitation electrons to ionization coefficient per unit length at the E-field direction,  $\mu$  is the photo absorption coefficient,  $x_1$  is the distance of the electron to cathode, and r is the function of  $r'$  and  $x_1$ . The initial voltage of streamer can be calculated from (4.7) using the method of annulus electric charge. The moving time of the electron in this process is equal to the distance divided by excursion velocity; the excursion velocity  $v_{e2}$  is a function of E-field and gas pressure,

$$v_{e2} = \left(2.74 \frac{E}{p} + 39.1\right) \times 10^3 \text{ m/s} \quad (4.8)$$

(3) Limited by the criterion of the tenable streamer in (4.7), the positive streamer may possibly arrive at the cathode or not. However, because of the fast development of this period, the time spent in this period can be neglected [21].

The electron avalanche will travel the distance of  $x$  and the streamer passing through the remaining distance  $(dg - x)$  (the scintling distance). What is clear here is that the time to breakdown is sum of times spent by electron avalanche and streamer. Summarizing the above analysis, the breakdown time  $t$  of the switch breakdown can be written as:

$$t = \frac{x}{v_{e1}} + \frac{dg - x}{v_{e2}} \quad (4.9)$$

where  $v_{e1}$  is the average velocity of the electron avalanche traveling the distance of  $x$  in gas with pressure  $p$  that in case of this thesis the gas is air in normal room (laboratory ) and  $v_{e2}$  is the average velocity of the streamer, which can be calculated from (4.8). Because of the enhanced effect, the E-field of the main gap  $E$  is

$$E = \frac{|U_g - Ut|}{dg} k \quad (4.10)$$

All the given equations are considered with some consumption that parameters that have known effect on the trigatron system are constant. For example, humidity in air for a trigatron system running in a normal air environment can change the operation of trigatron. Although that at least as an approximation, the given equations can be used.



## **5. AUTOMATION OF IMPULSE VOLTAGE GENERATOR**

### **5.1 Aim of Automation**

High voltage impulse tests are normally performed by the comparison method. Two or more impulse voltage and current records are compared with each other at different voltages. If they show no differences in the wave-shape then the insulation has passed the test. For such measurements, a highly accurate and disturbance-free measuring system is necessary. As an example in impulse test of a high voltage insulator depending on highest voltage that insulator can withstand for, in different voltage levels several test are demonstrated. In each voltage level several tests are done.

In high voltage laboratory of ITU some parts of impulse tests are done with a six stage impulse voltage generator which the generator is the subject of this thesis to be automated. During the automation one of the subjects is prepare, the generator as it can has same impulse voltage magnitude during the tests and even the output voltage to be free of disturbances.

As seen it was hard and even impossible to have same impulse voltage magnitude during tests. There were disturbances on the output voltage shape on front and peak. Therefore, we can list the objects of automation for the six stages impulse voltage generator in ITU High Voltage Laboratory as below:

- Achieve exact desired output impulse voltage magnitude
- Disturbance free output voltage shape

Typical operation of the impulse generator is successive switching of series capacitors of stages. The desired switching is started from first stage and simultaneously. When the first stage is triggered (by a trigatron), the remaining stages can be switched successively in series as a result of overvoltages originating from the voltage breakdown at the first spark gap. The level of the overvoltages on these spark gaps not yet fired was thus decisive for the successful series connection

of all capacitors. The parameters, which influence the overvoltages are in the main, the stray capacitance (earth and interstage capacitance) and the front and tail resistors. Here we can say some parts of the impulse voltage generator have two functions. One function is to generate and form the output voltage e.g. the lightning or switching impulse up to some million volts. The other function is to generate internal overvoltages to fire the spark gaps that have to make the series switching of the charged capacitors. However, here the attempt is to obtain triggering even without internal overvoltages.

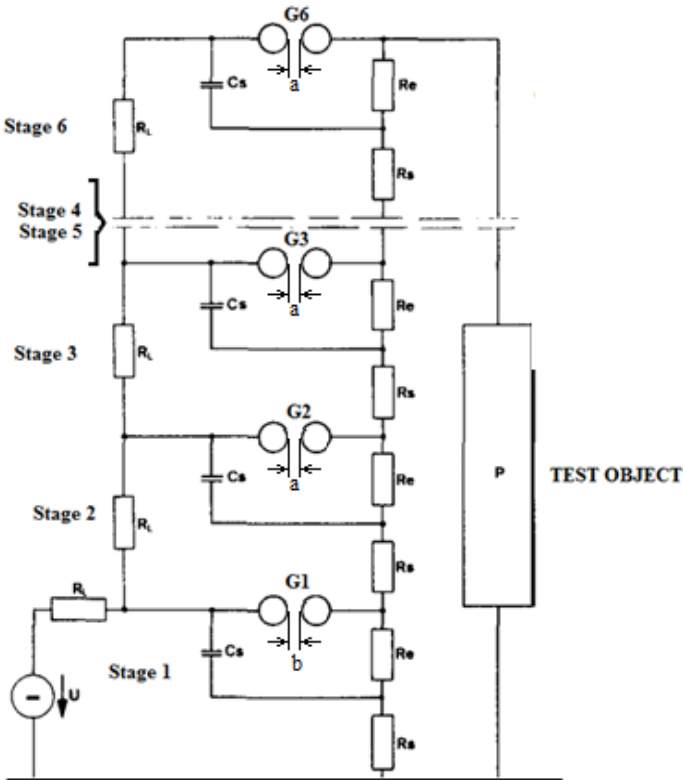


**Figure 5.1:** six stages Impulse voltage generator circuit.

Figure 5.1 shows a basic IVG circuit with six stages. When charging voltage  $U$  is applied, after a time interval (the charging time of capacitors) the spark gaps in stages ( $G_1, G_2 \dots G_6$ ) will discharge and thereby make the series connection of stage capacitors. With no external triggering mechanism, the spark gaps will discharge in their nature behavior. The instant that spark gaps discharge is influenced by some parameters such as distance between gaps of each stage, humidity and dirt in the air. Therefore, gaps may discharge at some random instants but not an exact point and it means different charging voltages. Since the output voltage magnitude is a ratio of

charging voltage  $U$ , we derive that the magnitude of output voltage will have a random tolerance over the exact voltage that we expect (we expect output voltage magnitude as a multiple of charging voltage  $U$  and stage number).

## 5.2 Definition of “ $u_{tr}$ ” Parameter

In ideal operation of the impulse voltage generator for a charging voltage value of  $U$ , we expect one output value. In disoperation of the generator with regarding random discharge of gaps, for a value of  $U$  we may have different impulse voltage magnitude. So on it can be resulted that controlling discharging of switching gaps will solve the problem. To control the discharges of gaps we used a triggering system (trigatron) that will be discussed in details.

Let us say that the self-firing voltage of the gaps is  $u_2$  (the charging voltage that switching gaps discharges by their nature). Then if before the charging voltage reaches  $u_2$  we trigger the switching gaps, successive discharges can be obtained. Figure 5.2 describes the setup for this.

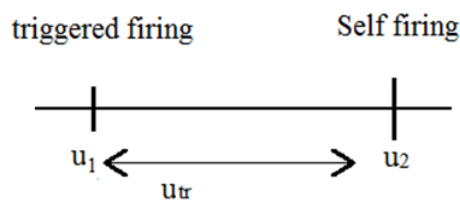


**Figure 5.2:** The definition of  $u_{tr}$  parameter.

In figure 5.2:

$u_1$  is triggering point (DC charging voltage) and  $u_1 < u_2$

$u_2$  is self-firing point (DC voltage of charger that causes spark gaps to fired)

$u_{tr}$  is the interval that we can fire the switching gaps.

As interval  $u_{tr}$  is long as flexible the triggering system is which that means with once adjusting charging unit of the generator and not changing gap distance we can obtain several output voltage magnitude. In not triggered generators, discharging is obtained by adjusting gap distance, which in the some percent's of changing voltage  $U$  it can be hard to have same output voltage in test purposes. Triggering system can result in gaining time and accuracy during tests.

**5.3 Proper Operation of IVG**

There are some requirements necessary for a series switching system to connect the charged capacitors in series for industrial testing with the standard lightning and switching impulse voltages that can be listed as below:

A mechanism, which can operate as independently as it, can operate of the charging voltage in the various ranges of that. Usually in lower charging voltages such mechanism could be miss operated.

A release working range that is large enough to facilitate the triggered firing sufficiently far below the static breakdown voltages of the spark gaps.

A switching spark gap with extremely long maintenance-free life i.e. reduced erosion. Over the time, the triggering voltage can cause damages on isolating parts of system that is on sphere.

A with range of firing possibility (wide  $u_{tr}$ ) demonstrates an acceptable system performance [40].

**5.4 Trigratron Setup for IVG**

The system used for triggering is trigratron that by using a high voltage impulse causes the spark switch to discharge. Figure 5.3 shows a schematic for trigratron. A resistor grounds the sphere that triggering system is installed. In the impulse generator under study only on first stage there is trigratron installed.

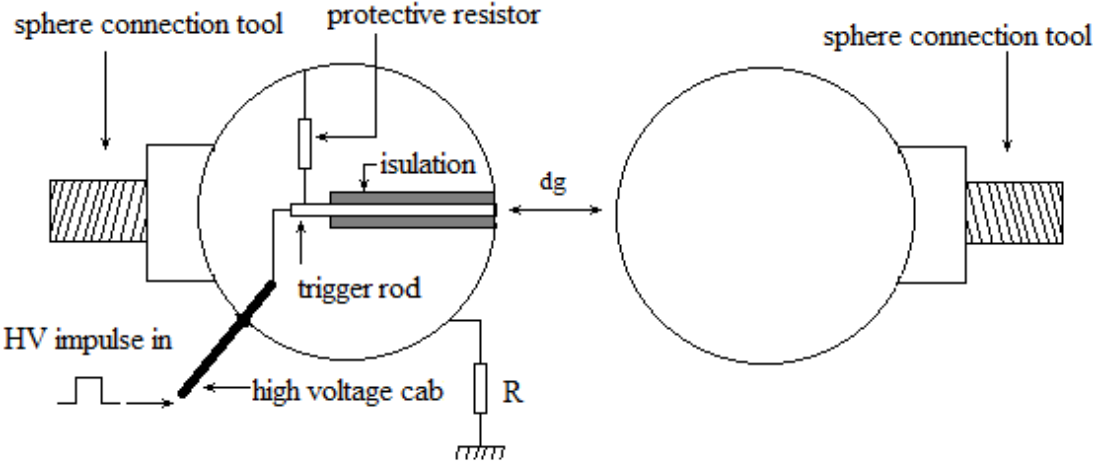


**Figure 5.3:** Side view of the trigratron spheres.



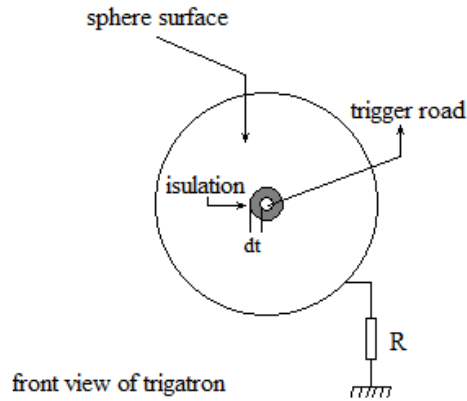


**Figure 5.4:** Front view of the trigatron sphere.

HV impulse input for the trigatron (shown in figure 5.3) is generated through a thyristor switched circuit.

### 5.5 Generation of Triggering Pulse

The principle of the circuit is charging and discharging of a capacitor in the primary terminals of high voltage transformer. The resulted impulse is then increased by transformer ratio to a high voltage impulse level. Through a high voltage cable, the HV impulse is carried to the trigger road in the sphere. When the HV impulse reaches edge point of trigger road (shown in figure 5.3), since the surface of the sphere is grounded (through a low value resistor) a spark forms between them and fires the switching spark gap (of the first stage). Figure 5.5 describes the impulse generating circuit.

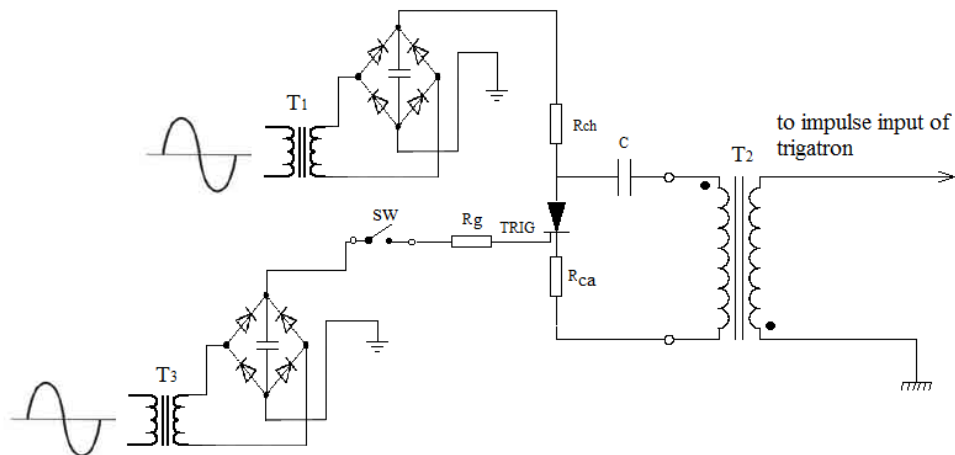


**Figure 5.5:** Trigger impulse generating circuit.

The capacitor C is charged to via T1 to a dc voltage of 150 V DC. The resistor  $R_{ch}$  controls charging time of C. when the capacitor is ready for discharge, closing switch sw fires the thyristor gate and puts the thyristor in conducting area and discharges the capacitor C through primary windings of transformer  $T_1$ . This produces the impulse wave of figure 5.6, which is the impulse needed to trigger the trigatron installed in impulse voltage generator. The input voltage of thyristor gate is supplied by  $T_3$  and is 12 V DC. Figure 5.6 and 5.7 show the circuit of figure 5.5 that installed in the laboratory and connected to the generator.



**Figure 5.6:** Triggering circuit (as schematic of figure 5.5).



**Figure 5.7:** Triggering circuit in connection with the IVG.

The circuit of figure 5.5 generates the impulse wave needed for the IVG. The output waveform of the triggering circuits is in figure 5.8.



**Figure 5.8:** Trigger impulse waveform.

## 5.6 Trigratron Test

As mentioned before the distance between stage spheres could affect the operation of impulse voltage generator. For successive discharging of spark gaps, it is necessary to have same spheres distances in stages except of first stage. In figure 5.1 the distance between spheres of the stages are shown as (a) for the first stage and (b) for other stages where difference between them is  $\Delta$  (i.e.  $\Delta = a - b$ ). Usually in the systems without trigratron system, to start the discharging of spark gaps from the first stage, the b is to be set smaller than a which means  $\Delta > 0$ . Adjusting this condition even if guaranties the successive discharging, finding optimum value of  $\Delta$ , in which the generator's output is standard impulse voltage and all the stages are discharged successively, leads to inflexible operation.

In presence of trigratron system,  $\Delta$  can be adjusted to the lowest value (i.e. close to 0). In the impulse voltage generator under study, during various tests we have figured out how the system function can be affected by the trigratron system. To show the relationships between parameters introduced in figure 5.2 some tests at charging ranges of 30 kV to 100 kV with 10 kV steps.

## 5.7 Tests Results

The tests are done for two different values of  $\Delta$  ( $\Delta_1 < \Delta_2$ ) to show the influence of  $\Delta$  with two polarities of charging voltage of the impulse voltage generator. The condition  $\Delta_1 < \Delta_2$ , means in  $\Delta_1$  the gap distance for first stage spheres is larger than that in  $\Delta_2$ . For each polarity by 10 kV steps starting from 30 kV the numerical value

for  $u_1$  (the threshold voltage of triggering by trigatron) for each step is achieved. The voltage of trigger pulse is 6 kV. The results are listed in tables.

**Table 5.1:** Test results for  $\Delta_1$  (positive polarity).

$u_2$ [kV]	$u_1$ [kV]	$u_{tr}$ [kV]
28.2	24.1	4.1
41.9	34.4	7.5
50	38.1	11.9
60.4	45.8	14.6
70.8	54.6	15.4
81.7	62.1	19.6
91	69	22
100.6	77.2	22.8

**Table 5.2:** Test results for  $\Delta_2$  (positive polarity).

$u_2$ [kV]	$u_1$ [kV]	$u_{tr}$ [kV]
28.2	25	3.2
41.9	36.7	5.2
50	43.6	6.4
60	53.1	6.9
70	61	9
79.5	66	13.5
90	75.9	14.1
100	83	17

**Table 5.3:** Test results for  $\Delta_1$  (negative polarity).

$u_2$ [kV]	$u_1$ [kV]	$u_{tr}$ [kV]
29.1	24.2	4.9
40.6	32	8.6
50	38.6	10.9
59.2	45.8	13.4
71.4	55.5	15.9
81.4	62.2	19.2
90.6	70	20.6
101.6	77.4	24.2

**Table 5.4:** Test results for  $\Delta_2$  (negative polarity).

$u_2$ [kV]	$u_1$ [kV]	$u_{tr}$ [kV]
29.2	26.1	3.1
40.9	36.7	4.2
50	43.6	6.9
61	53.1	7.9
71.2	61	10.2
80.5	66	14.5
91	75.9	15.1
100.7	83	17.7

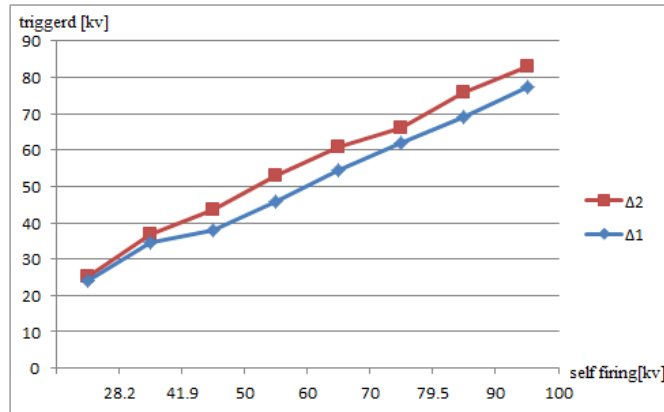


**Figure 5.9:** Comparison of  $\Delta_1$  and  $\Delta_2$  effect on  $u_{tr}$  range in presence of trigatron and positive polarity of the generator.

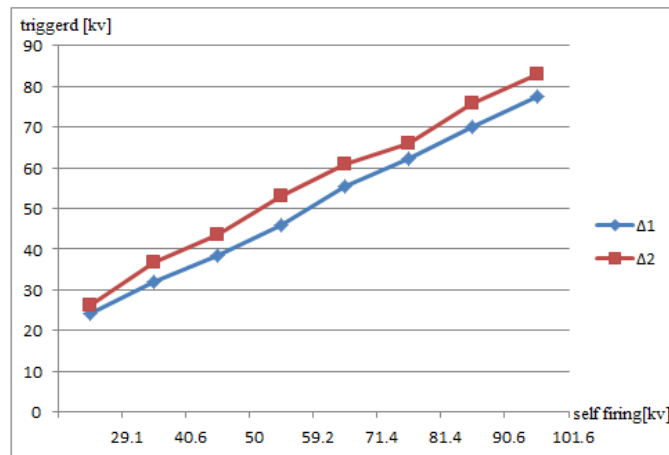


**Figure 5.10:** Comparison of  $\Delta_1$  and  $\Delta_2$  effect on  $u_{tr}$  range in presence of trigatron and negative polarity of the generator.

From test results in tables, 5.1 to 5.4 and the comparison of them in figures 5.9 and 5.10 it can be concluded in two aspects. First, the parameter  $u_{tr}$  is that makes the impulse generator able to produce various voltages ranges and it should be as wide as possible. Large value of  $u_{tr}$  means that operator of the generator can produce various output voltage magnitude with only once adjusting of DC charging unit. Secondly, the width of  $u_{tr}$  is a function of  $\Delta$  (since it will be showed that the magnitude and the energy of trigger pulse of trigatron have no effect on  $u_{tr}$ ). For two values of  $\Delta_1$  and  $\Delta_2$  while  $\Delta_1 < \Delta_2$  some tests are demonstrated that the result is larger  $u_{tr}$  for smaller  $\Delta$ .

As a practical example, it is to test a subject for its impulse behavior under 70 kV (=  $u_1$ ) in presence of trigatron system. When there is no trigatron system in the generator, we have to increase the DC charging of the generator and open the gap

distance in stages. Exactly achieving the 70 kV test voltage is hard to obtaining in this way. In presence of the trigatron we can set the self-firing voltage of the generator to arbitrary value of some kilo volts above 70 kV (like 80 kV). Since we can use  $u_{tr}$  width, if the self-firing occurs in 80 kV, then we have  $u_{tr} = 22$  kV. Therefore, we can fire the generator when the voltage is 70 kV. In this way, obtaining the same voltage will be possible. It was a practical interpretation use of results given in tables 5.1 to 5.4.

## 5.8 Trigger-Pulse Magnitude and Energy Effect on Trigatron Operation

### 5.8.1 Trigger Pulse Magnitude

To analysis, the effects of trigger pulse magnitude and energy on the overall system we can vary them in the circuit diagram of figure 5.5. The applied DC voltage comprised from  $T_1$  altered which that results on trigger impulse magnitude. For sake of magnitude we checked two various voltages, 6 kV and 12 kV. The tests performed for positive and negative working voltages of impulse generator and  $\Delta_1$ . Tables 5.5 and 5.6 show the results.

**Table 5.5:** Trigger pulse magnitude effect for 12 kV trigger pulse, positive polarity.

$u_2$ [kV]	$u_1$ [kV]	$u_{tr}$ [kV]
28.2	24.2	4.0
41.7	34.1	7.6
50	38.1	11.9
60.4	45.6	14.8
70.8	54.6	15.4
81.7	61.7	20
91	68.9	22.1
100.6	76.8	23.1

**Table 5.6:** Trigger pulse magnitude effect for 12 kV trigger pulse, negative polarity.

$u_2$ [kV]	$u_1$ [kV]	$u_{tr}$ [kV]
29.1	24.1	5
40.6	32	8.6
50	38.3	11.2
59.2	45.8	13.4
71.4	55.2	16.2
81.4	62.0	19.4
90.6	70.1	20.5
101.6	77.1	24.5

The comparison of tables 5.5 and 5.6 are demonstrated in figure 9.

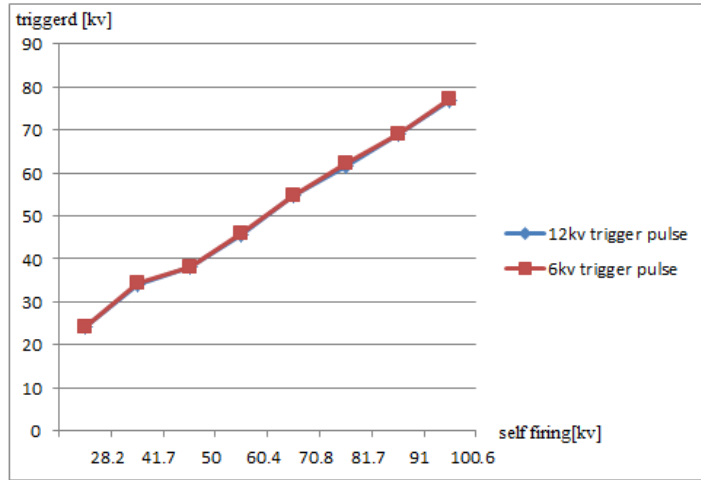


**Figure 5.11:** Comparison of trigger pulse voltage magnitude for 6 and 12 kV trigger pulse with  $\Delta_1$  and positive polarity of generator.

Comparison of result for 6 and 12 kV trigger pulse, shows a negligible effect on the width of  $u_{tr}$  (which is desired to be as wide as possible). Same result obtained for negative polarity of generator too. From this point it can be said that to prevent insulating material of trigger pin from failing and reducing electrical stress on it, it's better to keep the trigger pulse voltage on threshold value of it that in this case the is 6 kV.

### 5.8.2 Trigger Pulse Energy

The value of capacitor C on circuit diagram of figure 5.5, defines the energy of applied trigger pulse. To investigate how this energy affects the  $u_{tr}$  some tests are done with various capacitors and trigger pulse magnitude of 6 kV. The results are given in tables 5.7 to 5.10.

**Table 5.7:** Trigger impulse energy analysis, 6 kV trigger pulse, 1  $\mu$ F and positive.

$u_2$ [kV]	$u_1$ [kV]	$u_{tr}$ [kV]
28.2	24.1	4.1
41.7	34.3	7.4
50	38.2	12.1
60.4	45.3	15.1
70.8	54.6	15.4
81.7	61.5	20.2
91	68.9	22.1
100.6	76.5	23.4

**Table 5.8:** Trigger impulse energy analysis, 6 kV trigger pulse, 8.2  $\mu\text{F}$ , and positive polarity.

$u_2$ [kV]	$u_1$ [kV]	$u_{tr}$ [kV]
28.2	24.1	4.1
41.7	34.1	7.6
50	38.2	12.1
60.4	45.1	15.3
70.8	54.6	15.4
81.7	61.4	20.3
91	68.7	22.3
100.6	76.6	23.0

**Table 5.9:** Trigger impulse energy analysis, 6 kV trigger pulse, 1  $\mu\text{F}$ , negative polarity.

$u_2$ [kV]	$u_1$ [kV]	$u_{tr}$ [kV]
29.1	24.3	4.7
40.6	32	8.6
50	38.2	11.3
59.2	45.7	13.5
71.4	55.3	16.1
81.4	61.9	19.5
90.6	70.1	20.5
101.6	77.3	24.3

**Table 5.10:** Trigger impulse energy analysis, 6 kV trigger pulse, 8.2  $\mu\text{F}$ , and negative polarity.

$u_2$ [kV]	$u_1$ [kV]	$u_{tr}$ [kV]
29.1	24.0	5.1
40.6	32.2	8.4
50	38.3	11.2
59.2	45.7	13.5
71.4	55.2	16.2
81.4	62.0	19.4
90.6	70.1	20.5
101.6	77.1	24.5

The transferred energy produced by 1  $\mu\text{F}$  and 8.2  $\mu\text{F}$  capacitor for both positive and negative polarities of impulse voltage generator are applied and the results from tables 5.7 to 5.10 are compared in figures of 5.10 and 5.11.



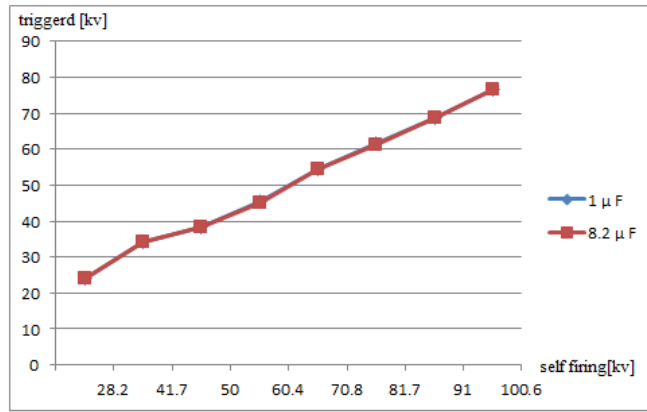


**Figure 5.12:** Comparison of trigger pulse energy effect on  $u_{tr}$  for, 6 kV trigger pulse, positive polarity.

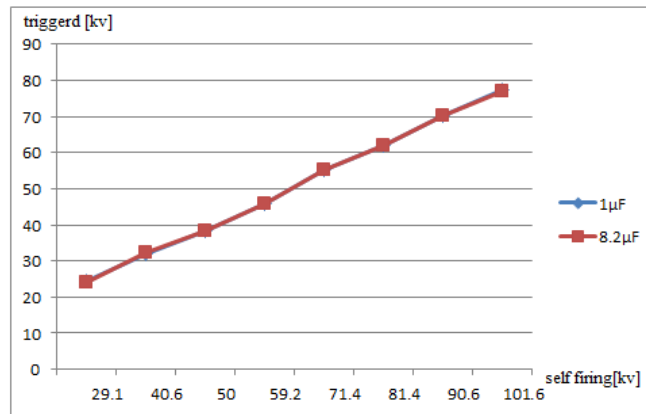


**Figure 5.13:** Comparison of trigger pulse energy effect on  $u_{tr}$  for, 6 kV trigger pulse, negative polarity.

As it is understandable from tables 5.7 to 5.10 and the comparison of results in figures 5.12 and 5.12, varying trigger pulse energy had negligible effect on  $u_{tr}$  of the trigatron.

For both polarities on the main gap, using a range of steep fronted long-tailed trigger pulses with 6 and 12 kV peak, negligible change in working range or in time lag to breakdown of trigatron occurred.

The energy of the trigger pulse was also varied, using a constant voltage pulse of 6 kV peak with a range of discharge capacitances of 1 and 8.2  $\mu\text{F}$  again the change in working range and time lag to breakdown was found to be negligible since  $u_{tr}$  was approximately constant.

## 5.9 Unit Step Response of Impulse Voltage Divider

Measuring system of impulse voltage generator at High Voltage Laboratory of ITU consists of a 3 meter height voltage divider and a digital oscilloscope. The output of the divider is connected to the oscilloscope via a coaxial cable. The divider is able to work in full and half measuring possession that enables it to have more accuracy in measuring various impulse ranges.

To evaluate the transfer characteristics of the divider, unit step response of it is considered. The configuration of test setup is as figure below.

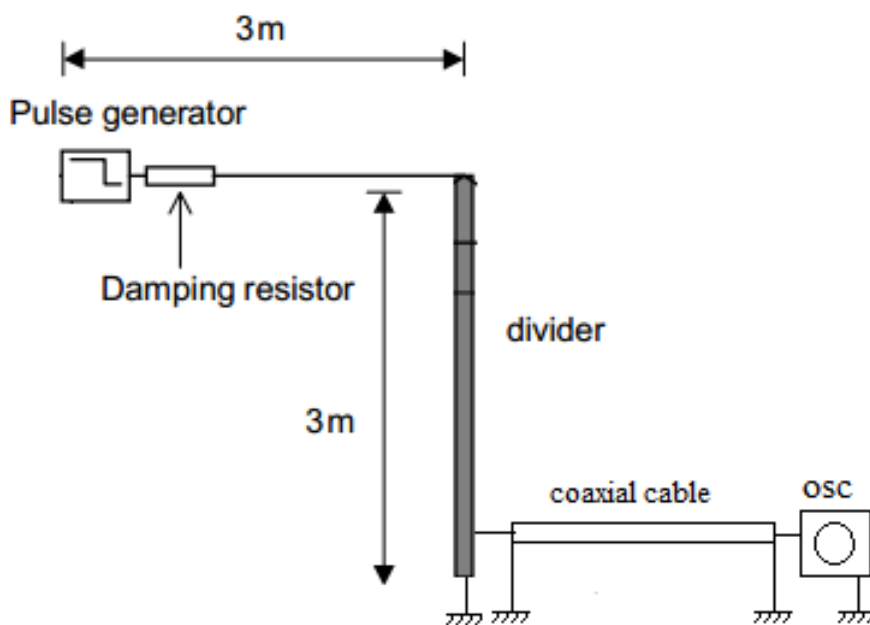


**Figure 5.14:** Unit step response setup.

To reduce inductances, low inductance wide copper bands are used. To measure output wave shapes, a 200 MHz oscilloscope is used. Pulse generator is a combination of mercury relay with a DC source. Mercury relays can close the circuit with lowest disturbances caused from contactors impact, since this connection is made by absorbing mercury in both contact. The rise time of the generated unit step pulse is 33 ns with 158 V magnitudes (figure 5.13).

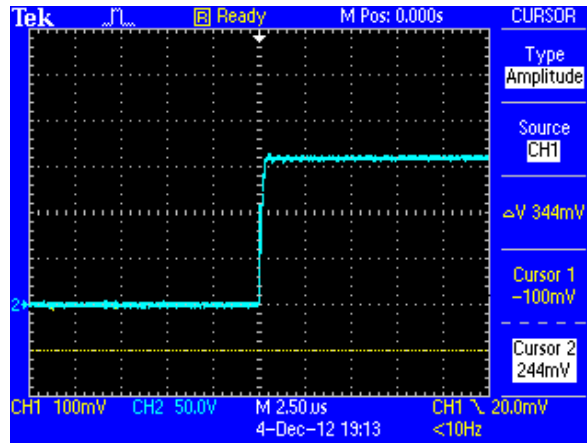


**Figure 5.15 :** Applied unit step impulse waveform.

The lead between the generator and the impulse voltage divider should be involved in calculations of unit step response too. The resistor  $R_d$  is used with 0, 50 and 100 ohm, to see how the lead may affect the output waveform. The lead damps the oscillations. Unit step response is evaluated for both full and half divider in presence of these damper resistor values.

### 5.9.1 Full divider unit step response

In full dividing position, the divider can measure voltages up to one MV. The divider ratio and its transfer characteristics are considered here.

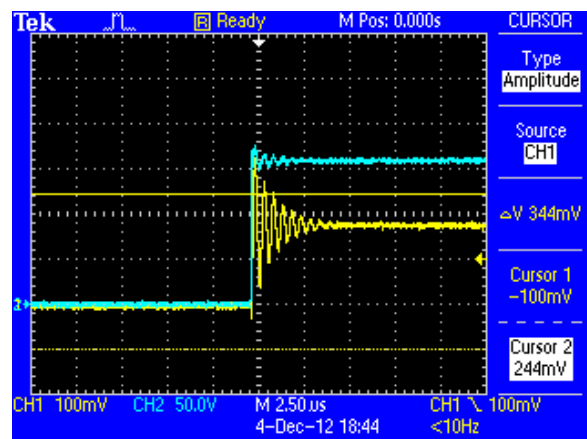


**Figure 5.16:** Unit step response of full divider,  $R_d = 0$ .

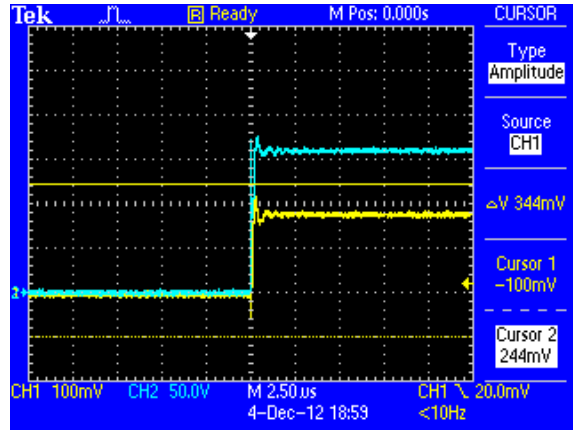


**Figure 5.17:** Unit step response of full divider,  $R_d = 50 \Omega$ .

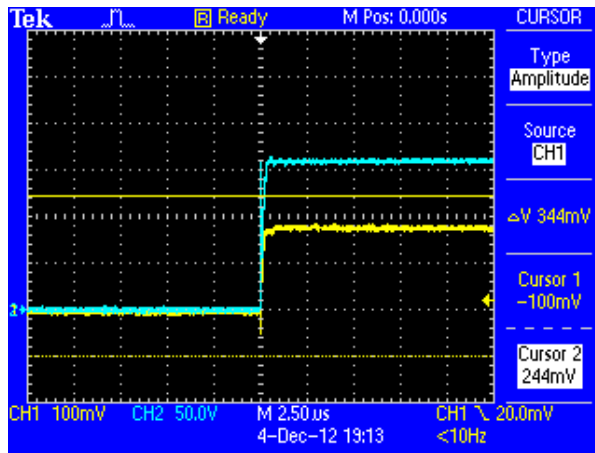


**Figure 5.18:** Unit step response of full divider,  $R_d = 100 \Omega$ .

To consider the transfer characteristics of the full divider as mentioned in chapter three, we have calculated the  $T_\alpha$ ,  $T_n$ ,  $T_s$ ,  $T$  and  $\beta$  parameters. Regarding the formulas described in chapter three some codes are written in MATLAB to calculate the parameters. Table 5.11 shows the values of the parameters.

**Table 5.11:** Unit response parameters of full divider.

$R_d$ [ $\Omega$ ]	$T_\alpha$ [ns]	$T_n$ [ns]	$T_s$ [ns]	$T$ [ns]	$\beta$ [%]
0	47	35	78	41	80
50	61	59	127	56	22
100	73	72	178	73	1

From the unit response full divider ratio can be calculated. The settled output voltage is 176 mV. From there:

$$V_o = 176 \text{ mV}$$

$$V_i = 158 \text{ V}$$

$$\text{Then ratio} = V_i / V_o = \frac{158 \text{ V}}{176 \text{ mV}} = 898$$

### 5.9.2 Half Divider Unit Step Response

Same unit response evaluation is carried out for half divider and same parameters calculated for half divider.

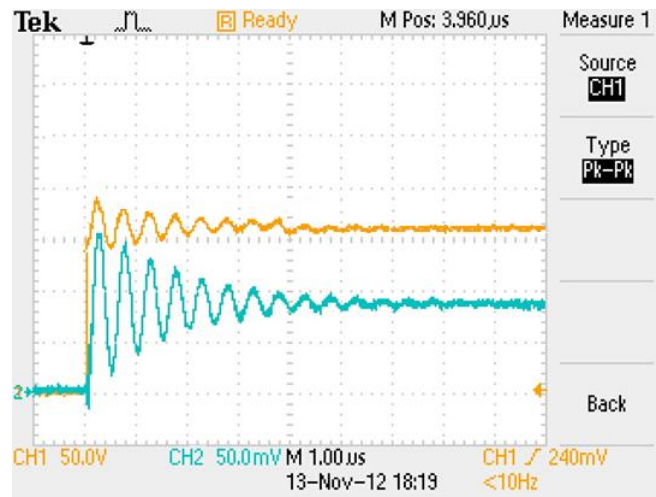


**Figure 5.19:** Unit step response of half divider,  $R_d = 0 \Omega$ .

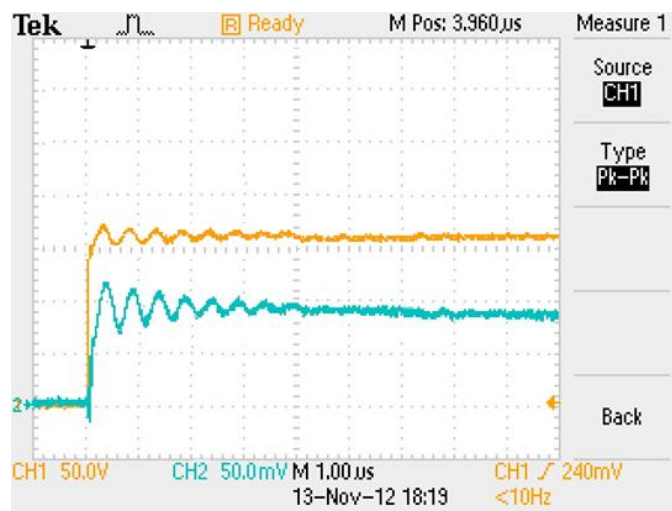


**Figure 5.20:** Unit step response of half divider,  $R_d = 50 \Omega$ .

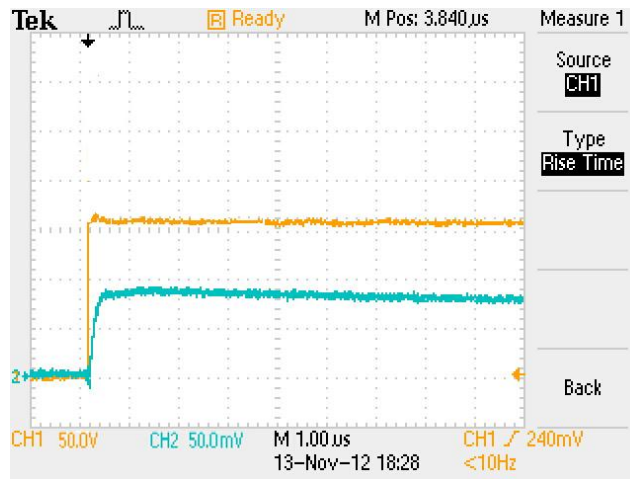


**Figure 5.21:** Unit step response of half divider,  $R_d = 100 \Omega$ .

Transfer characteristic parameters for half divider are given in table 5.12. Same codes in MATLAB are used to these calculations too.

**Table 5.12:** Unit response parameters of half divider.

$R_d$ [ $\Omega$ ]	$T_\alpha$ [ns]	$T_n$ [ns]	$T_s$ [ns]	$T$ [ns]	$\beta$ [%]
0	28	25	80	43	75
50	45	39	119	51	24
100	62	62	145	65	1

Half divider ratio is calculate as:

$$V_o = 346 \text{ mV}$$

$$V_i = 158 \text{ V}$$

$$\text{Then ratio} = V_i / V_o = \frac{150 \text{ v}}{346 \text{ mv}} = 456$$

## 6. CONCLUSION

The thyristor controlled triggering system that installed on IVG of ITU High Voltage Laboratory, had acceptable performance on tests that have done. The generated impulse voltage can be controlled on favorable values. There are some considerations that some of them effect the trigger system's performance and some do not. The magnitude of triggering impulse tested for 6 kV and 12 kV and the energy of the trigger impulse tested for two values. It was shown that in both tests the parameter  $u_{tr}$  was constant. Thus it can be said that increasing the magnitude and the energy of triggering impulse after a threshold value have no effects on system performance. Therefore, to prevent trigatron sphere insulator from further electrical field stress, it is better to keep it on it's lowest value. Larger electrical stress on trigatron sphere insulator can damage it. Defining the parameter  $u_{tr}$ , helps the operator of the generator in control room to adjust the desired voltage level in an easier way.

Unit step response of the impulse voltage divider in ITU High Voltage Laboratory is evaluated. According to IEC standards there are some recommended limits for these parameters. Table 6.1 shows the recommended limitations.

**Table 6.1:** Recommended response parameters for impulse voltage reference measuring systems. (IEC standard 600602-2010)

Voltage	Recommendations for		
	Full and tail-chopped lightning impulses	Front-chopped lightning impulses	Switching impulses
Experimental response time $T_N$	$\leq 15$ ns	$\leq 10$ ns	-
Settling time $t_s$	$\leq 200$ ns	$\leq 150$ ns	$\leq 10$ $\mu$ s
Partial response time $T_\alpha$	$\leq 30$ ns	$\leq 20$ ns	-

The results of the USR parameters calculated for full and half divider in tables 5.11 and 5.12 are compared with IEC recommendation in table 5.13. In case of full divider, the settling time  $t_s$ , is within the recommended limitation ( $t_s \leq 200$  ns). The

experimental responstime,  $T_n$  and partial response time,  $T_\alpha$ , have some deviation from IEC recommended limitations. In precense damping resistor,  $R_d$ , the overshoot,  $\beta$ , is acceptable and when  $R_d = 100 \Omega$ , the overshoot is close to zero.

In case of half divider, the calculated parameters fit the recommended limitation better than full divider. The settling time,  $t_s$ , is less than 200 ns. Experimental response time and partial response time have less deviation from IEC recommended limitations.

The lead impedance is involved in forming the generated lightning or switching impulse and damping the oscillations on output lightning impulse. In the unit step response analysis we saw that the lead impedance can alter some parameters of the output waveform. Therefore, in defining the lead impedance it must be considered to give a optimum value to satisfy all limitations.



## REFERENCES

- [1] **Łukasz Staszewski.** (2001). Lightning Phenomenon – Introduction and Basic Information to Understand the Power of Nature.
- [2] **Skuletic, S.D.; Mijajlovic, P.** (2003). Experimental Investigations of Switching Overvoltages in 110 kV Network of Power System of Montenegro. *PowerTech Conference Proceedings, 2003 IEEE Bologna: Vol. 2.*
- [3] **Carsimamovic.** (2005). Modeling and Calculation of Switching Overvoltages in 400 kV Electrical Networks. *Computer as a Tool, 2005. EUROCON 2005. The International Conference on: Vol. 2, pp. 1521 – 1521.*
- [4] **Andrew R. Hileman.** (1999). Insulation Coordination for Power Systems. New York: Marcel Dekker, c1999
- [5] **E. Kuffel, W. S. Zaengl, J. Kuffel.** (2000), High Voltage Engineering Fundamentals. Oxford; Boston : Butterworth-Heinemann, 2<sup>nd</sup> edition 2000.
- [6] **M. S. Naidu.** (1996). High Voltage Engineering. New York: McGraw-Hill, c1996. 2<sup>nd</sup> edition.
- [7] **Dieter Kind.** (1978). An introduction to high-voltage experimental technique, by Willey, textbook for electrical engineers.
- [8] **K. Feser.** (1971). A new type of voltage divider for the measurement of high impulse and ac voltages. <[www.haefely.com/pdf/scientific/e1-12.pdf](http://www.haefely.com/pdf/scientific/e1-12.pdf)>, Switzerland.
- [9] **K. Feser, M. Modrusan.** (2011). Actual problems and limitations in measurements with impulse voltage dividers in the multi-megavolt range. <[www.haefely.com/pdf/scientific/e1-47.pdf](http://www.haefely.com/pdf/scientific/e1-47.pdf)>, Switzerland.
- [10] **K.Feser, E. Gockenbach.** (1988). Distortion-free measurement of high impulse voltages. *Power Delivery, IEEE Transactions on: Vol. 3, pp. 857 – 866.*
- [11] **Stephen A. Dyer.** (2001). Wiley Survey of Instrumentation and Measurement. Wiley Encyclopedia of Electrical and Electronics Engineering, *department of Electrical and Computer engineering, Kansas State University, John Wiley & Sons, Apr 7, 2004.*
- [12] **J. Rungis, K. Schon.** (1988). The evaluation of impulse divider response parameters. *Power Delivery, IEEE Transactions on: Vol. 3, pp. 88 – 95.*
- [13] **Hylten-Cavallius, N. Chagas.** (1983). A New Approach to Minimize Response Errors in the Measurement of High Voltage Impulses. *Power Engineering Review, IEEE: Vol. PER-3, pp. 34-3.*

- [14] **Yi Liu; Fuchang Lin; Guan Hu.** (2011). Design and Performance of a Resistive Divider System for Measuring fast HV Impulse. *Instrumentation and Measurement, IEEE Transactions on: Vol. 60, pp. 996 – 1002.*
- [15] **Peterkin and P. F. Williams.** (1988). Physical Mechanism of Triggering in Trigatron Spark Gap. *Applied Physics Letters: Vol 53, pp 182 – 184.*
- [16] **F. Williams and F. E. Peterkin.** (1989). Triggering in trigatron spark gaps: A fundamental study. *Journal of applied physics science, Vol. 66, pp. 4163 – 4175.*
- [17] **I. H. Mitchell, P. Choir J. M. Bayley.** (1995). Optimization of a High-Voltage Trigatron Switch. *Journal of applied physics science: Vol. 78, pp. 3659 – 3664.*
- [18] **Li Cai, Lee Li, Fuchang Lin.** (2012). Analysis on Triggering and Discharge Characteristics of Three-Electrode Trigatron Gap. *IEEE TRANSACTIONS ON PLASMA SCIENCE: Vol. 40, pp. 1634 – 1642.*
- [19] **A. M. SLETTEN, Sivilingenior, M.N.I.F.** (1957). Characteristics OF the Trigatron Spark-Gap. *Proceedings of the IEE - Part C: Monographs: Vol. 104, pp. 54 – 64.*
- [20] **H. Zhu, L. Huang, Z. H. Cheng, J.** (2009). Effect of the gap on discharge characteristics of the three-electrode trigatron switch. *American Institute of Physics: Vol. 105, pp. 113303 – 113305.*
- [21] **A. Rodewald, K. Feser.** (1974). The generation of lightning and switching impulse voltages in the UHV region with an improved Marx circuit. *Power Apparatus and Systems, IEEE Transactions on: Vol. PAS-93, pp. 414 – 420.*
- [22] **IEC 60060-2 (2010).** High-voltage test techniques – part 2: Measuring systems, edition 3.0, 2010-11, IEC, Geneva, Switzerland

## **CURRICULUM VITAE**



**Name Surname:** Farid ABDOLALIZADEHGHAREHVERAN

**Place and Date of Birth:** IRAN

**Address:** AZERBAIJAN-GHARBI MIYANDOAB

**E-Mail:** farid.zade2@gmail.com

**B.Sc.:** Azad University

**Professional Experience and Rewards:**

Project manager in Promer Engineering Co.

Electrical Engineer in Yashil Tavan Gostaran Azarbayjan